Modelling of Geotechnical Problems using Soft Computing

A Thesis Submitted in Partial Fulfillment of the Requirements for the

Degree of

Master of Technology

in

Civil Engineering

SUNIL KHUNTIA

DEPARTMENT OF CIVIL ENGINEERING

NATIONAL INSTITUTE OF TECHNOLOGY, ROURKELA

2014

Modelling of Geotechnical Problems using Soft Computing

A Thesis Submitted in Partial Fulfillment of the Requirements for the

Degree of

Master of Technology

in

Civil Engineering

Under the guidance and supervision of

Prof. Chittaranjan Patra

Submitted By

Sunil Khuntia

(ROLL NO. 212CE1023)

DEPARTMENT OF CIVIL ENGINEERING

NATIONAL INSTITUTE OF TECHNOLOGY, ROURKELA

2014

CERTIFICATE

This is to certify that the thesis entitled "**Modelling of Geotechnical Problems using Soft Computing**" being submitted by **Sunil Khuntia** in partial fulfillment of the requirements for the honor of **Master of Technology Degree** in **Civil Engineering** with specialization in Geotechnical Engineering at National Institute of Technology, Rourkela, is an authentic work completed by him under my guidance and supervision.

To the best of my knowledge, the matter exemplified in this report has not been submitted to any other university/institute for the award of any degree or diploma.

Place: Rourkela
Date:

Prof. Chittaranjan Patra
Department of Civil Engineering
N I T, Rourkela

ACKNOWLEDGEMENT

I earnestly express my profound feeling of appreciation to my thesis supervisor, Prof. Chittaranjan Patra for his master direction, constant support and spark all around the course of postulation work. I am genuinely grateful for his educated backing and imaginative feedback, which headed me to create my thoughts and made my work fascinating and agreeable.

I might additionally want to express my profound thankfulness and earnest because of Prof. N. Roy, Head, Civil Engineering Department, Prof. S.P. Singh, Prof. S. K. Das and Prof. R. N. Behera of Civil Engineering for giving different varieties of conceivable help and consolation. I am obliged to every one of them and NIT Rourkela for providing for me the essentials and opportunity to execute them.

I want to take this probability to thank my parents and my sister for their unconditional love, moral support and encouragement for the completion of this specific project.

I ought to express my genuine because of all my nearby companions and seniors in light of their ethical backing and advices throughout my M-Tech project.

Sunil Khuntia

Table of Contents

Abstract

Correlations are very significant from the earliest days; in some cases, it is essential as it is difficult to measure the amount directly, and in other cases it is desirable to ascertain the results with other tests through correlations. Soft computing techniques are now being used as alternate statistical tool, and new techniques such as artificial neural networks (ANN), support vector machine (SVM), multivariate adaptive regression splines (MARS) has been employed for developing the predictive models to estimate the needed parameters. In this report, four geotechnical problems like compaction parameters of sandy soil, compression index of clay, relative density of clean sand and side resistance of drilled shaft have been modeled. In the first problem, compaction parameters (i.e. MDD and OMC) of sandy soil have been predicted from its index properties such as coefficient of uniformity, percentage of sand and fines content with reference to compactive effort and MARS shows better predictability. In the second problem, the relative density (D_r) of clean sand has been predicted from coefficient of uniformity, mean diameter of grain size with reference to four levels of compactive effort and predictability of LS-SVM is found to be very accurate. In third problem, compression index of clay has been predicted from consistency limits, natural moisture content and initial void ratio and the developed ANN shows better prediction. In the fourth problem, side resistance of drilled shaft has been predicted from effective stress and undrained shear strength and the MARS model performs better than the other models. Various error criteria such as mean absolute error (MAE), root mean square error (RMSE), mean absolute percentage error (MAPE) and correlation coefficient (R) have been considered for the comparison of different models. Finally different sensitivity analysis has been shown to identify the significance of different input parameters that affects the developed models. The performance comparison showed that

the soft computing system is a good tool for minimizing the uncertainties in the soil engineering projects. The use of soft computing may provide new approaches and methodologies to minimize the potential inconsistency of correlations.

List of Figures

List of Tables

CHAPTER 1
INTRODUCTION

1.1 Introduction

In geotechnical engineering, empirical connections are frequently used to evaluate certain engineering properties of soils. By means of data from extensive laboratory or field testing, these correlations are generally derived with the help of statistical methods. Artificial neural networks (ANNs), support vector machine (SVM) and multivariate adaptive regression splines (MARS) are the forms of artificial intelligence. These techniques learn from data cases presented to them in order to capture the functional interactions among the data even if the fundamental relationships are unknown or the physical meaning is tough to explain. This is in contrast to most traditional empirical and statistical methods, which need prior information about the nature of the relationships among the data. AI is thus well suited to model the complex performance of most geotechnical engineering materials which, by their very nature, exhibit extreme erraticism. This modeling capability, as well as the ability to learn from experience, have given AI superiority over most traditional modeling approaches since there is no need for making assumptions about what the primary rules that govern the problem in hand could be.

ANN is still considered as 'black box' system with poor simplification, though various efforts made for modification and explanations. Recently support vector machine (SVM), based on statistical learning theory and structural risk minimization is being used as an alternate prediction model. The SVM uses constrained minimization, penalizing the error margin during training. The error function being a convex function better generalization used to observe in SVM compared to ANN.

Though AI techniques has proved to have the superior predictive capability than other traditional methods for modeling complex performance of geotechnical engineering

materials, still it is facing some criticism due to the lack of transparency, knowledge extraction and model uncertainty. To overcome this there is a development of improvised AI techniques.

1.2 Origin of Project

- Empirical relationships are frequently used to estimate certain engineering properties of soils in geotechnical engineering.
- Computational techniques learn from data samples presented to them in order to capture the functional relationships among the data even if the fundamental relationships are unknown or the physical sense is difficult to clarify.
- Most traditional empirical and statistical methods need prior knowledge about the nature of the interactions among the data.
- Soft-computing techniques are suitable to model the complex behavior of most geotechnical engineering materials which exhibit extreme inconsistency.

1.3 Objective

- To apply various soft-computing techniques like ANN, MARS and SVM in parametric estimation of Geotechnical problems.
- To model for relative density of granular soil from grain size distribution and compaction energy.
- To model for compaction parameters (Maximum Dry Density and Optimum Moisture Content) of granular and c-ϕ soils from index properties and compaction energy.
- To model for compression Index from various physical properties of clayey soil.
- To model the side resistance of drilled shaft from effective stress and undrained shear strength.
- To compare the efficiency of different models..

1.4 Applications in Geotechnical Engineering

Various geotechnical problems where soft computing has been applied are:

- For forecasting the axial and lateral load capacities in compression and uplift of pile foundations.
- Conventional constitutive modeling based on the elasticity and plasticity theories to properly simulate the performance of geomaterials.
- For estimating several soil properties including the shear strength, stress history, pre-consolidation pressure, swell pressure, compaction and permeability, soil classification and soil density.
- Predicting liquefaction potential.
- Bearing capacity and Settlement prediction of shallow foundations.
- Other applications of Artificial Intelligence in geotechnical engineering include retaining walls, dams, blasting, mining, geo-environmental engineering, rock mechanics, site characterization, tunnels and underground openings and slope stability.

1.5 Methodology for Soft-Computing

- **Artificial Neural Network (ANN)**
  - A universal function approximator and fast to evaluate new examples.
- **Multivariate Adaptive Regression Splines (MARS)**
  - Capacity to find complex data mapping and produce simple, easy-to-interpret models.
- **Support Vector Machine**
  - The quality of generalization and ease of training of SVM is better.

1.6 Software used

For the above modeling MATLAB R2008b has been used.

CHAPTER 2
METHODOLOGY

2.1 Artificial Neural Network (ANNs)

2.1.1 An overview of ANNs

In the last decades, Artificial Intelligence (AI) techniques such as Artificial Neural Networks (ANNs) have received a great deal of attention. In essence, ANN is an information technology that mimics the human brain and nervous system in learning from experience and generalizes from previous examples to generate new outputs by abstracting essential characteristics from inputs in the pattern of variable interconnection weights among the processing elements. ANNs are more powerful than traditional methods in the situations when the problem requires qualitative or complex quantitative reasoning where the conventional statistical and mathematical methods are inadequate or the parameters are highly interdependent and data is intrinsically noisy, incomplete or error prone (Bailey and Thompson, 1990).

ANNs have many advantages over traditional methods of modeling. Firstly, as opposed to the traditional mathematical and statistical methods, ANNs are data-driven self-adaptive methods, which can capture subtle functional relationships among the data even if the underlying relationships are unknown or hard to describe. Secondly, ANNs are able to capture complex nonlinear relationship with better accuracy (Rumelhart et al. 1994). Thirdly, the most important advantage of ANNs over mathematical and statistical models is their adaptability. ANN systems can automatically adjust their weights to optimize their behavior (Boussabaine, 1996). Neural networks have been utilized for classification, clustering, vector quantification, pattern association, function approximation, control, optimization and search.

2.1.2 Basic Concepts of ANNs

An artificial neural network is a computational model defined by four parameters: type of neurons, connection architecture, learning algorithm and recall algorithm (Mehrotra, et al., 1997).

2.1.2.1 Artificial Neural Systems

ANNs is an information processing technology that simulates the human nervous system. It is built on three basic components: *processing elements (PE)* which are an artificial model of human neuron, *interconnections* whose functions are similar to the axon and *synapses* which are the junctions where an interconnection meets a PE. Each PE receives signals from other PEs that constitute an input pattern. This input pattern stimulates the PE to reach some level of activity. If the activity is strong enough, the PE generates a single output signal that is transmitted to other PEs through an interconnection.

2.1.2.2 Processing Elements

Figure 1 describes a typical artificial neuron. The input signals come from either the environment or outputs of other PEs and form an input vector:

$$A=(a_1,.....,a_i,.....a_n) \tag{1.1}$$

Where, a_i is the activity level of the i_{th} PE or input. There are weights bound to the input connections: $w_1, w_2, ..., w_n$. The neuron has a bias b. The sum of the weighted inputs and the bias form the net input signal, X:

$$X = b_j + \sum_{i=1}^{n} w_{ij}\, a_i = W \times A + b \tag{1.2}$$

The input signal is then sent to a transfer function, which serves as a non-linear threshold. The transfer function calculates output signal of the PE (j) as:

$$O_j = f(X) \tag{1.3}$$

Where O_j is the output signal from PE(j); f is a transfer function and X is the net input signal to PE(j).

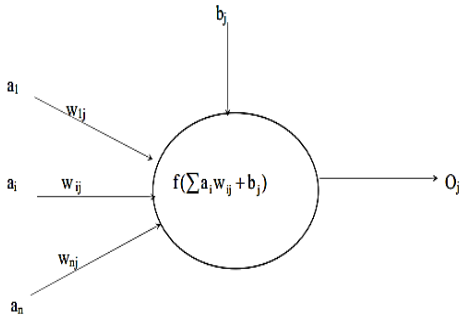

Figure 2.1 Generic processing element of neural network

2.1.2.3 Threshold functions

There are many threshold functions adopted in ANNs. The two most commonly used transfer functions are linear and sigmoid.

- The *linear threshold function*: f(x) = x
- *The sigmoid function*: *Log-sigmoid transfer function* and *Tan-Sigmoid transfer function* is commonly used in backpropagation networks, partly because in backpropagation, it is important to be able to calculate the derivatives of any transfer function used (Demuth and Beale, 2000). They can be expressed as the following equations:

Logistic function: $f(x) = \frac{1}{1+e^{-x}}$

Hyperbolic tangent: $f(x) = \frac{e^{x} - e^{-x}}{e^{x} + e^{-x}}$

2.1.2.4 Architecture of ANNs

The architecture of an ANN is the organization that assembles PEs into layers and links them with weighted interconnections. The architecture determines how computations proceed. A common ANN architecture is determined by three distinguishing characteristics: connection types, connection schemes and layer configurations.

The most commonly used ANN paradigm is multilayer perceptions (MLPs). A MLP consists of an input layer, at least one hidden layer and one output layer. The neurons in each layer are usually fully connected to the neurons in another layer. Among them, three-layer feed forward network is the most popular. Feed forward network is a type of network in which connection is allowed from a node in layer i only to nodes in layer i+1. The three layers are input layer, hidden layer and output layer. Input layer is the layer that receives input signals from the environment. Output layer is the layer that emits signals to the environment. Hidden layers are layers between the input and output layers.

2.1.2.5 Learning Rules

Learning makes possible modification of behavior in response to the environment. A learning rule is a procedure for modifying the weights of connections between the nodes and biases of a network. These are three broad learning categories: supervised learning, unsupervised learning and reinforcement learning.

2.1.3 ANN Model Equation

A model equation is developed using the weights from trained neural network model (Goh et al. 2005). The mathematical equation relating input parameters to output parameter can be written as

$$y = f_n \left\{ b_0 + \sum_{k=1}^{h} \left[w_k \; f_n \left(b_{hk} + \sum_{i-1}^{m} w_{ik} \; X_i \right) \right] \right\} \tag{1.4}$$

where y = predicted value of output, f_n = transfer function, h = no. of neurons in the hidden layer, X_i = value of Inputs, m= no of input variables, w_{ik} = connection weight between i_{th} layer of input and k_{th} neuron of hidden layer, w_k = connection weight between k_{th} neuron of hidden layer and single output neuron, b_{hk} = bias at the k_{th} neuron of hidden layer and b_0 = bias at the output layer.

2.1.4 Methodology of ANN

The sequences of modeling by ANN are given in the flow chart below.

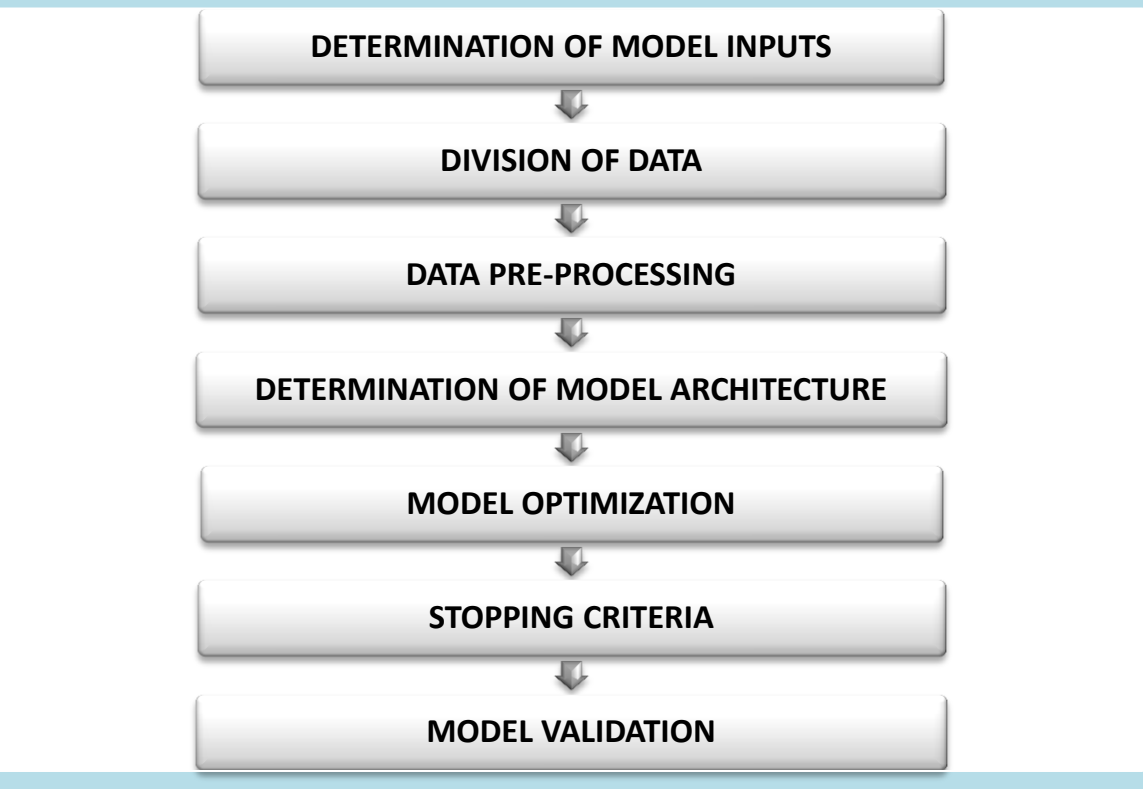

Figure 2.2 Flow chart of neural network modelling

2.1.4.1 Determination of Model Inputs

A subset of input variables can significantly improve model performance. A large number of input variables usually increase the network size, resulting in a decrease in processing speed and a reduction in the efficiency of the network. Another approach is to train with different combinations of input variables and to select the network that has the best performance. The network that performs the best is then retained. This process is repeated for an increasing number of input variables, until the addition of other variables results in no improvement in model performance.

2.1.4.2 Division of Data

ANNs accomplish best when they do not generalize beyond the range of the data used for standardization. Therefore, the purpose of ANNs is to non-linearly introduce (generalize)

in high-dimensional space between the data used for calibration. A discrete validation set is needed to ensure that the model can generalize within the range of the data used for calibration. It is common practice to split the existing data into two subsets; a training set, to construct the neural network model, and an independent validation set to evaluate the model performance. Usually, two-thirds of the data are suggested for model training and one-third for validation.

2.1.4.3 Data Pre-processing

Once the presented data have been divided into their subsets (i.e. training, testing and validation), it is significant to pre-process the data in a appropriate form. Data pre-processing is necessary to ensure all variables obtain equal attention during the training process and it usually speeds up the learning process. Pre-processing can be in the form of data scaling, normalization and transformation. Scaling the output data is essential, as they have to be equal with the limits of the transfer functions used in the output layer (e.g. between –1.0 to 1.0 for the tanh transfer function and 0.0 to 1.0 for the sigmoid transfer function). In some cases, the input data need to be normally distributed in order to obtain optimal results. To improve the performance, transformation of the input data can be done to some known forms (i.e. linear, log, exponential, etc.).

2.1.4.4 Determination of model architecture

Determining the network architecture is most essential and difficult job in ANN model development. It needs selection of the ideal number of layers and the number of nodes. It is usually achieved by fixing the number of layers and choosing the number of nodes in each layer. For MLPs, there are always two layers signifying the input and output variables in any neural network.

2.1.4.5 Model optimization

The process of improving the connection weights is known as training or learning.

The aim is to find a global solution to what is usually a highly non-linear optimization problem. The technique most commonly used for finding the optimum weight grouping of feed-forward MLP neural networks is the back-propagation algorithm.

2.1.4.6 Stopping criteria

Stopping criteria are used to adopt when to break the training process. They determine whether the model has been optimally or sub-optimally trained. Training can be stopped: after the performance of a fixed number of training records; when the training error reaches an effectively small value; or when no or minor changes in the training error occur.

2.1.4.7 Model Validation

Once the training segment of the model has been effectively accomplished, the performance of the trained model should be validated. The purpose of the model validation phase is to confirm that the model has the ability to simplify within the limits set by the training data. The error criteria such as coefficient of correlation (R), the root mean squared error (RMSE), and the mean absolute error (MAE) are often used to evaluate the performance of models. The coefficient of correlation is a measure that is used to determine the relative correlation and the goodness-of-fit between the expected and experimental data.

2.2 Details of Support Vector Machine (SVM)

2.2.1 Support Vector Machine (SVM)

SVM has been utilized to solve a regression problem. Let us consider a training set $(x_1, y_1), (x_2, y_2).....(x_N, y_N)$ from a vector, $x_i \in \mathrm{R}^n$ with corresponding targets y_i, $i = 1, 2, \ldots, N$. ε-SVR determines a linear function defined on x_i as,

$$f(x) = (w, x) + b \tag{1.5}$$

where w is a high-dimensional weight vector and b ∈ R as the bias such that there is

at most ε distance from the actual data and f (X) should be flat. (.) denotes the dot product. No care is taken as long as errors are less than ε. But, any deviation more than ε is not accepted. Flatness means the value of w should be as small as possible. This can be written as convex optimization problem:

$$Minimize \frac{1}{2}\|w\|^2$$

$$\text{Subjected to } \begin{cases} y_i - \langle w, x_i \rangle - b \leq \varepsilon \\ \langle w, x_i \rangle + b - y_i \leq \varepsilon \end{cases}$$

In this case it is assumed that a function $\boldsymbol{f}$ exists which approximates the data set (x_i, y_i) with ε precision. Introducing slack variables ξ_i, ξ_i^* the problem can be stated as,

$$\text{Minimize } \frac{1}{2}\|w\|^2 + C\sum(\xi_i + \xi_i^*) \tag{1.6}$$

$$\text{Subjected to } \begin{cases} y_i - \langle w, x_i \rangle - b \leq \varepsilon + \xi_i \\ \langle w, x_i \rangle + b - y_i \leq \varepsilon + \xi_i \\ \xi_i, \xi_i^* \geq 0 \end{cases}$$

The parameter C controls the trade-off between the flatness of $\boldsymbol{f}$ and tolerance level of error ε. This deals with a ε-insensitive loss function expressed as,

$$|\xi|_\varepsilon = \begin{cases} 0, if\ |\xi| \leq \varepsilon \\ |\xi| - \varepsilon, otherwise \end{cases}$$

The graphical presentation of the ε-insensitive loss function is shown in the Figure 2.3. The optimization problem defined in (6) is easily solved in its dual formulation. The dual optimization problem can be written as ,

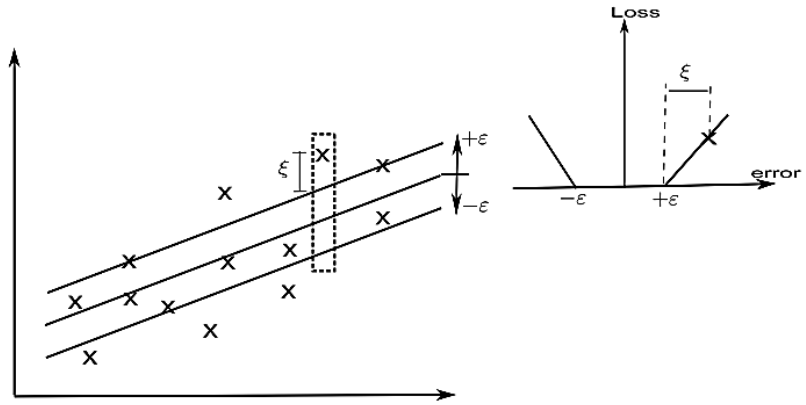

Figure 2.3 Soft margin loss setting for a linear SVM

$$\text{Maximize}\begin{cases} -\frac{1}{2}\sum(\alpha_i-\alpha_i^*)(\alpha_j-\alpha_j^*)\langle x_i,x_j\rangle \\ -\varepsilon\sum(\alpha_i+\alpha_i^*)+\sum y_i(\alpha_i-\alpha_i^*) \end{cases} \tag{1.7}$$

$$\text{Subjected to } \sum(\alpha_i-\alpha_i^*)=0 \text{ and } \alpha_i,\alpha_i^*\in[0,C]$$

where are α_i, α_i^* Lagrange multipliers. In the above equations x_i and x_j are input vector spaces.

To address nonlinear regression problems, the linear SVR is prolonged to nonlinear SVR by mapping the input space into a high dimensional feature space through a kernel function $\varphi(x)$. In such case, (x, x^t) is replaced by $k(x, x^t)$. Distinctive kernel functions used in the SVR are RBF, polynomial, linear and defined as,

Polynomial Kernel

In machine learning, the **polynomial kernel** is a kernel function commonly used with support vector machines (SVMs) and other kernelized models, that represents the similarity of vectors (training samples) in a feature space over polynomials of the original variables, allowing learning of non-linear models. Intuitively, the polynomial kernel looks not

only at the given features of input samples to determine their similarity, but also combinations of these.

For degree-*d* polynomials, the polynomial kernel is defined as

$$K(x,y)=(x^T y+c)^d \tag{1.8}$$

where x and y are vectors in the input space, i.e. vectors of features computed from training or test samples. $c \geq 0$ is a constant trading off the influence of higher-order versus lower order terms in the polynomial. When c = 0, the kernel is called homogenous. (A further generalized poly-kernel divides $x^T y$ by a user-specified scalar parameter a.)

As a kernel, K corresponds an inner product in a feature space based on some mapping φ:

$$K(x,y)=\langle \varphi(x), \varphi(y) \rangle$$

The nature of φ can be glanced from an example. Let d = 2, so we get the special case of the quadratic kernel. Then

$$K(x,y)=\left(\sum_{i=1}^{n} x_i y_i + c\right)^2 = \sum_{i=1}^{n} x_i^2 y_i^2 + \sum_{i=2}^{n} \sum_{j=1}^{i-1} \sqrt{2x_i y_i}\sqrt{2x_j y_j} + \sum_{i=1}^{n} \sqrt{2cx_i}\sqrt{2cy_i} + c^2 \tag{1.9}$$

Radial Basis Function Kernel

In machine learning, the (**Gaussian**) radial basis function kernel, or **RBF kernel**, is a popular kernel function used in support vector machine classification.

The RBF kernel on two samples **x** and **x'**, represented as feature vectors in some ***input space***, is defined as

$$K(x,x') = \exp\left(-\frac{\|x-x'\|_2^2}{2\sigma^2}\right) \tag{1.10}$$

where $\|x-x'\|_2^2$ may be recognized as the squared Euclidean distance between the two feature vectors. σ is a free parameter. The parameter σ in represents the spread of Gaussian kernel.

An equivalent, but simpler definition involves a parameter $\gamma = -\frac{1}{2\sigma^2}$:

$$K(x, x') = \exp(\gamma \|x - x'\|_2^2) \tag{1.11}$$

Since the value of the RBF kernel decreases with distance and ranges between zero (in the limit) and one (when **x** = **x'**), it has a ready interpretation as a similarity measure. The feature space of the kernel has an infinite number of dimensions; for $\sigma = 1$, its expansion is:

$$\exp\left(-\frac{1}{2}\|x - x'\|_2^2\right) = \sum \frac{(x^T x')^j}{j!} \exp\left(-\frac{1}{2}\|x\|_2^2\right) \exp\left(-\frac{1}{2}\|x'\|_2^2\right) \tag{1.12}$$

2.2.2 Least Square Support Vector Machine (LS SVM)

LSSVM models are an alternate formulation of SVM regression (Vapnik and Lerner, 1963) proposed by Suykens et al. (2002). Consider a given training set of N data points $\{x_k, y_k\}_{k=1}^N$ with input data $x_k \in R^N$ and output $y_k \in r$ where R^N the N-dimensional vector space is and r is the one-dimensional vector space. For prediction of output using multiple parameters, $x = [inputs]$ and $y = [output]$.

In feature space LSSVM models take the form

$$y(x) = w^T \varphi(x) + b \tag{1.13}$$

Where the non-linear mapping $\varphi(.)$ maps the input data into a higher dimensional feature space; $w \in R^n; b \in r; w$ = an adjustable weight vector; b = the scalar threshold. In LSSVM for function estimation the following optimization problem is formulated:

$$\text{Minimize: } \frac{1}{2} w^T w + \gamma \frac{1}{2} \sum_{k=1}^{N} e_k^2$$

$$\text{Subjected to: } y(x) = w^T \varphi(x_k) + b + e_k, k = 1, ..., N \tag{1.14}$$

Where e_k = error variable and γ = regularization parameter. The following equation

for output prediction has been obtained by solving the above optimization problem (Scholkopf and Smola, 2002; Vapnik, 1988).

$$C_c = y(x) = \sum_{k=1}^{N} \alpha_k \, K(x, x_k) + b \tag{1.15}$$

$$\text{Where } K(x_k, x) = \exp\left[- \frac{\|x_k - x\|^2}{\sigma^2} \right] \text{ , k = 1,……..,} N \tag{1.16}$$

σ is the width of radial basis function and α_k is the Lagrange multiplier.

In LS-SVM regression algorithm, the regularization parameter γ and RBF kernel parameter σ^2 have to be tuned in order to achieve an accurate solution. An integrated parameter optimization approach via simplex i.e. multidimensional unconstrained non-linear optimization (Nelder and Mead 1965) and 10 fold cross-validation is used to minimize generalization error. The optimum values of parameters [γ, σ^2] and bias values have been used for the models developed herein.

2.3 Multivariate Adaptive Regression Splines (MARS)

MARS is a non-parametric regression technique introduced by Friedman (1991). It essentially detects relation between a dependent variable and a set of predictors by fitting piecewise linear regressions. In particular, MARS builds flexible models by dividing the whole space of each covariate into various subsets and then defining a different regression equation for each area. In this way, separate regression slopes in distinct intervals of the predictors space are individuated (Hastie et al. 2009). A key concept is the notion of knots that are the points that bound each interval of data in which a distinct regression equation is calculated, i.e. where the behavior of the modelled function changes.

In this way, the space of predictors is split into several regions in which truncated spline functions or basis functions (BFs) are fit. A truncated BF consists of a left-sided (1.17) and a right-sided (1.18) segments defined by a knot t:

$$b_q(x \quad t)=[\quad (x \quad t)]_+^q=\begin{cases}(t \quad x)^q, & \text{if} \quad x<t \\ 0 & \text{otherwise}\end{cases} \tag{1.17}$$

$$b_q^+(x \quad t)=[+(x \quad t)]_+^q=\begin{cases}(x \quad t)^q, & \text{if} \quad x<t \\ 0 & \text{otherwise}\end{cases} \tag{1.18}$$

where $b_q^-(x-t)$ and $b_q^+(x-t)$ are the BFs describing the regions to the left and the right of the knot t, q indicates the power (>0) to which the BFs are raised in order to manipulate the degree of smoothness of the resultant regression models. The general MARS model equation is given as

$$y_p=\alpha_0+\sum_{m=0}^{M}\alpha_m B_m(x) \tag{1.19}$$

where y_p is the dependent variable predicted through the MARS model, M is the number of BFs included into the model, α_0 is the constant term, α_m is the coefficient of the m^{th} truncated BF and $B_m(x)$ is the m^{th} truncated BF that may be a single spline function or a product (interaction) of two or more spline functions.

The optimal MARS model is built by a two-stage process: a forward selection procedure followed by a backward-pruning procedure. The forward procedure starts with just the constant term in the model and then, by an iterative way, selects the best pairs of BFs that improves the global model. This forward stepwise selection of BFs leads to a very complex and over fitted model that has poor predictive abilities for new data. So, in the backward stage, the "lack of fit" criterion is used to evaluate the contribution of each BF to the descriptive abilities of the model and the BFs with the lowest contribution are removed one at a time.

The "lack of fit" criterion used by MARS is the generalized cross-validation (GCV) criterion, i.e. the mean square error divided by a penalty dependent on the model complexity. It is given by:

$$GCV(M) = \frac{1}{n} \frac{\sum_{i=1}^{n} (y_i - y_p)^2}{\left[1 - \frac{C(M)}{n}\right]^2} \quad (1.20)$$

Where n is the number of observations in the data set, M is the number of non-constant BFs, and C(M) is the cost-complexity measure of the model containing M BFs. C(M) increases with the number of BFs and has the purpose to penalize model complexity in order to avoid over-fitting. It is defined as:

$$C(M) = M + d \times M \quad (1.21)$$

Where d is a cost penalty factor for adding a BF. The higher value of d reduces the number of BFs in the final model.

2.4 Performance criteria

The present study uses various statistical error measure criterions like R, MAPE and RMSE to compare different developed models. A good model should have; R value (expresses degree of similarity between predicted and actual values) close to 1 and low MAPE and RMSE values (indicate high confidence in model-predicted values).

Root mean-squared error (*RMSE*) is used to compute the square error of the prediction compared to actual values as well as the square root of the summation value. Thus the RMSE is expressed using the following equation:

$$RMSE = \sqrt{\frac{1}{n} \sum_{i=1}^{n} (y_p - y)^2} \quad (1.22)$$

Mean Absolute Percentage Error (MAP*E*) is a measure of closeness of predictions to actual values. The mean absolute error is given by

$$MAPE = \frac{1}{n} \sum_{i=1}^{n} \left(\frac{y_p - y}{y} \right)^2 \times 100 \quad (1.23)$$

The Coefficient of correlation (*R*) value is a measure of linear relationship between the predictions and the actual values. The R value is calculated using the following formula:

$$R=\frac{n(\sum y.y_p)-(\sum y)(\sum y_p)}{\sqrt{[n\sum y^2-(\sum y)^2][n\sum {y_p}^2-(\sum y_p)^2]}} \tag{1.24}$$

Mean of the observed data = $\bar{y}=\frac{1}{n}\sum_{i=1}^{n}(y_i)$

Total sum of squares = $SS_{total}=\sum_{i=1}^{n}(y_i-\bar{y})^2$

Explained sum of squares = $SS_{reg}=\sum_{i=1}^{n}(y_{pi}-\bar{y})^2$

Residual sum of squares = $SS_{residual}=\sum_{i=1}^{n}(y_i-y_p)^2$

Coefficient of determination (R^2) = $1-\frac{SS_{residual}}{SS_{total}}$

where y and y_p are the actual and the predicted values; $\bar{y}$ and $\bar{y}_p$ are average of the actual and the predicted values respectively; n is the sample size.

2.5 Sensitivity analysis

Different methods have been adopted for knowing the importance of the input parameters for the developed models.

2.5.1 Variance based sensitivity analysis

Iman and Hora (1990) investigate the performance of a sensitivity measure based on the percentage variance in *f* explained by any variable Xi. This technique is known as measure of importance, and its use is associated with the estimation of the quantity

$$S_i=\frac{Var_{xi}\left[E(f|X_i)\right]}{Var(f)} \tag{1.25}$$

where $E(f|X_i)$ indicates the expectation value of *f* when the i^{th} variable is fixed to the value X_i, $Var_{xi}[\bullet]$ stands for the variance of the argument over all the possible values of X_i and Var(*f*) is the unconditional (total) variance of *f*. In the present paper, the outcomes in the *f* are observed by keeping mean of the X_i value fixed for other arguments varying.

2.5.2 Rate of change of input

The sensitivity tests are carried out to determine the relative significance of each of the inputs and to find the inputs that affect the models performance. The sensitivity test is carried out on the all data by varying each of the input, one at a time, at a constant rate of 20%. For every input, the percentage change in the output is observed. The sensitivity (*S*) of each input is calculated by the following:

$$S = \frac{1}{N}\sum\left(\frac{\%\ \text{change in output}}{\%\ \text{change in input}}\right)\times 100 \tag{1.26}$$

where *N* = number of datasets used in the study.

2.5.3 Connection weight approach

Calculates the product of the raw input-hidden and hidden-output connection weights between each input neuron and output neuron and sums the products across all hidden neurons (Olden and Jackson, 2002b).

2.5.4 Garson's algorithm

Partitions hidden-output connection weights into components associated with each input neuron using absolute values of connection weights (Garson, 1991).

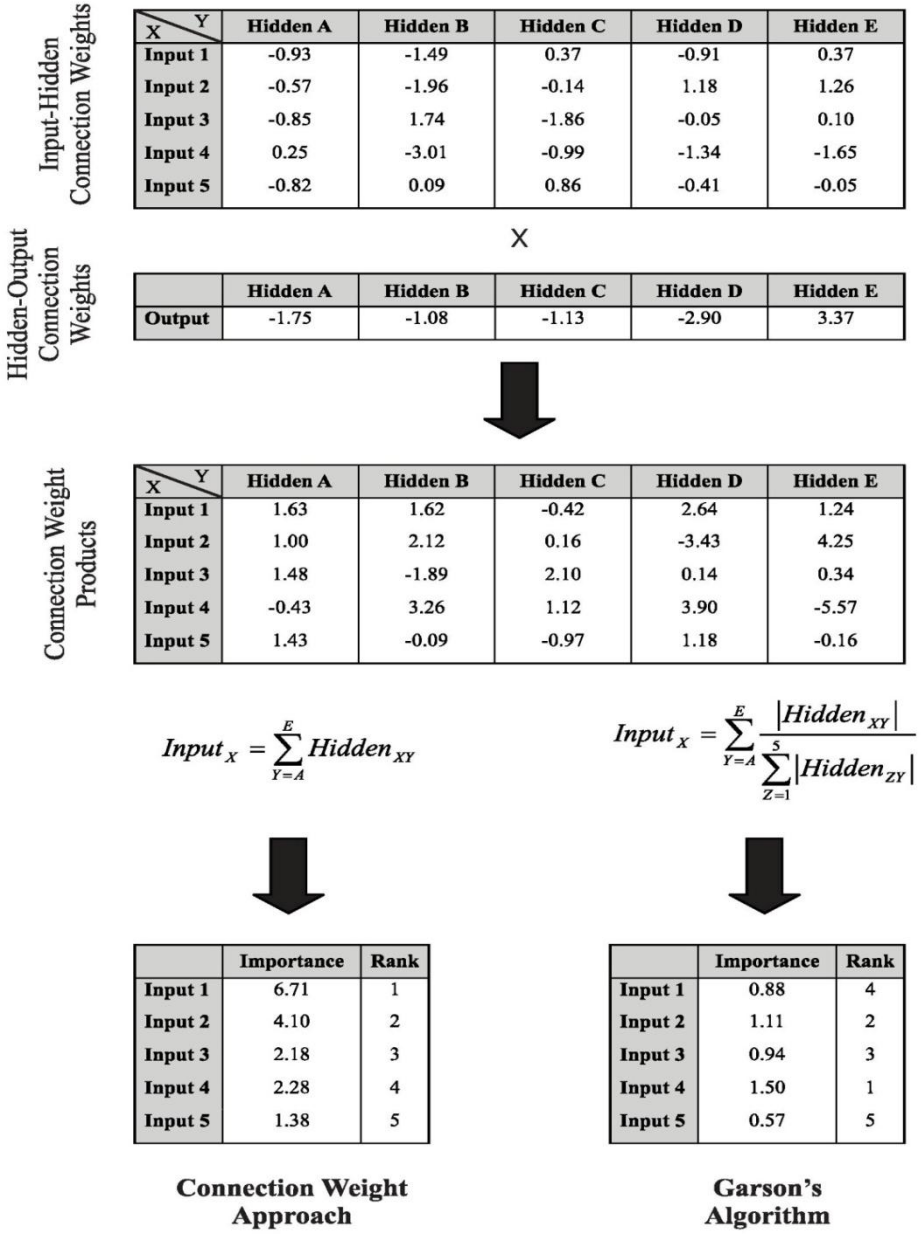

Figure 2.4 Steps for connection weight approach and Garson's algorithm (Olden, Joy and Death, 2004)

Sensitivity analysis is performed for choice of important input variables. Different methodologies have been recommended to select the important input variables. Goh (1994) and Shahin et al. (2002) have used Garson's algorithm (Garson, 1991) in which the input hidden and hidden output weights of trained ANN model are segregated and the absolute values of the weights are taken to select the significant input variables, and the details with

example have been presented in Goh (1994). It does not provide evidence on the effect of input variables in terms of direct or inverse relation to the output. Olden et al. (2004) suggested a connection weight approach based on the Neural Interpretation Diagram (NID), in which the actual values of input hidden and hidden output weights are taken. It sums the products across all the hidden neurons, which is defined as S_i. The relative inputs are corresponding to absolute S_i values, where the most important input corresponds to highest S_i value. The details of connection weight approach are presented in Olden et al. (2004).

CHAPTER 3
PREDICTION OF COMPACTION PARAMETERS OF SANDY SOIL

3.1 Introduction

Compacted soils are used in many projects such as highway embankments, railway subgrades, airfield pavements, earth dams and landfill liners. The granular materials are generally used as fill material in earth work. In the field, soils are usually compacted using rollers and other various equipments. To evaluate compaction in the field, laboratory compaction parameters are required using the Standard Proctor and Modified Proctor compaction which requires large efforts and time. A standard amount of compactive effort is applied to produce soil density with which site values can be compared. The compaction parameters of soils are influenced by many factors such as water content, compactive effort, and index properties. For a certain compactive effort, a typical compaction curve that relates the water content of the soil to its dry unit weight is usually obtained. The most important point on the compaction curve is the optimum compaction point in which two important parameters, maximum dry unit weight (MDD) and optimum water content (OMC), are obtained, and they represent compaction behavior.

In recent years attempts have been made to correlate Index properties of soil and gradation to obtain MDD and OMC of compacted sandy soils. Several researches have been done to correlate compaction parameters with index properties of fine-grained soils (Wang and Huang1984; Blotz et al.1999; Nagaraj et al. 2006; Sivrikaya et al. 2008; Sivrikaya 2008). On the other hand, prediction models of coarse-grained soils are rare (Korfiatis and Manikopoulos 1982; Omar et al. 2003). In recent years, Artificial Intelligence (AI) has been applied successfully to several problems in geotechnical engineering. Several soft-computing methods like Artificial Neural Network (ANN), Support Vector Machine (SVM), Genetic Programming (GP), Adaptive Neuro Fuzzy Inference System (ANFIS), Regression Tree,

Multivariate Adaptive Regression Splines (MARS) are continuously used in modeling of geotechnical problems. These techniques have been used for predicting the bearing capacity of piles, permeability of compacted clay liners, settlement prediction of shallow foundations on granular soils, swelling pressures of soil, compaction parameters of soils, slope reliability analysis, ultimate capacity of driven piles in cohesionless soils, OCR prediction of clay.

This study investigates the capability of ANN, MARS and LSSVM for determination of compaction parameters of coarse-grained soils with an emphasis on the influence of soil properties and compaction effort. MARS is a flexible, more accurate, and faster simulation method for both regression and classification problems (Friedman, 1991). Different models has been developed and observed that MARS gives a better predictability as compared to regression equation and other non-linear models from ANN and MARS.

The laboratory experiment was conducted by Mujtaba et al. (2013) for the determination of compaction parameters, grain size distribution and Index properties of sandy soil. The compaction parameters were determined at different compaction energy (*CE*) level (592 kN-m/m^3 & 2696 kN-m/m^3) and performing regression analysis, the potential input parameters were identified which affect the output parameters. Based on the analysis a regression model equation was developed for MDD and OMC. The model equations were as follows:

$$\begin{aligned} MDD(kN/m^3) &= 4.49\log(C_u) + 1.51\log(CE) + 10.2 \\ \log(OMC)(\%) &= 1.67 - 0.193\log(Cu) - 0.153\log(CE) \end{aligned} \tag{3.1}$$

where C_u = coefficient of uniformity

From the cross-correlation matrix, it is observed that two other parameters also affect the compaction parameters i.e. fines (%) and Sand (%) along with C_u and *CE*. In the present study, two models were taken into consideration consisting of the index properties and compaction energy. The inputs of the two models are as follows:

Model – I *Cu, CE*

Model – II Fines (%), Sand (%), C_u, *CE*

Model-III: Fines (%), Sand (%), D_{50}, C_u, *CE*

The data available in literature (Mujtaba et al., 2013) are taken with input and output parameters. The total number of data points considered is 220 out of which 160 are taken for training and 60 are taken for testing. Some of the data base of the experiment has been shown in Table 3.1 and the maximum, minimum, average, and standard deviation for the data used are shown in Table 3.2 and it can be seen that it covers a wide range of values. The successful application of a method depends upon the identification of suitable input parameters. Table 3.2 shows the cross correlation between the inputs and output; it can be seen that fines (%), sand (%), D_{50}, C_u and *CE* are found to be important input parameters for predicting *MDD* and *OMC*.

Table 3.1. some of the compaction of test data and index properties of soil

Sample No.	Gravel (%)	Sand (%)	Fines (%)	D_{60} (mm)	D_{50} (mm)	D_{30} (mm)	D_{10} (mm)	*MDD* (m) (kN/m^3)	*OMC* (m) (%)	*MDD* (s) (kN/m^3)	*OMC* (s) (%)
1	0	67	33	0.12	0.1	0.06	0.0319	18.2	11	17.2	14
2	3	64	33	0.15	0.11	0.06	0.014	20.1	9	19.1	12
3	0	91	9	0.11	0.1	0.09	0.075	16.3	13	15.4	16.5
4	0	92	8	0.11	0.1	0.09	0.075	16.0	13.5	15.2	16.5
5	2	82	16	0.2	0.17	0.1	0.06	17.9	12	17.0	16
6	0	84	16	0.2	0.17	0.1	0.04	18.1	11.5	17.1	15
7	4	68	28	0.27	0.2	0.08	0.024	20.0	8	18.9	11
8	0	70	30	0.21	0.19	0.08	0.02	20.0	9	18.9	11.5
9	2	70	28	0.22	0.19	0.08	0.019	20.4	9.5	19.3	12
10	0	57	43	0.16	0.1	0.055	0.021	20.0	9.5	18.9	12
11	0	96	4	0.12	0.11	0.1	0.08	16.3	14.5	15.4	18
12	0	94	6	0.11	0.1	0.09	0.08	16.2	15.5	15.4	18
13	0	92	8	0.7	0.58	0.27	0.085	19.8	11	18.8	12.5
14	0	92	8	0.17	0.14	0.1	0.075	16.3	14	15.6	17.5
15	3	52	45	0.16	0.09	0.04	0.017	20.4	9.5	19.5	10.5
16	2	79	19	0.21	0.19	0.1	0.05	18.2	10	17.3	12.5
17	2	72	26	0.2	0.18	0.09	0.045	18.9	11	18.1	14
18	0	83	17	0.21	0.2	0.15	0.05	17.9	11	17.0	14
19	0	54	46	0.15	0.095	0.058	0.027	19.0	9	18.1	12
20	0	71	29	0.2	0.16	0.08	0.021	19.2	9	18.2	12
21	2	74	24	0.2	0.16	0.09	0.038	18.5	9	17.6	11
22	3	77	20	0.195	0.15	0.092	0.05	17.6	11	16.7	14
23	2	60	38	0.15	0.11	0.06	0.026	18.8	9.5	17.9	12

24	5	50	45	0.12	0.09	0.05	0.026	19.0	9	18.1	11
25	0	83	17	0.21	0.19	0.11	0.05	17.4	11.5	16.6	15
26	0	86	14	0.27	0.21	0.17	0.051	17.9	13	16.8	16
27	0	94	6	0.21	0.2	0.14	0.08	17.7	12	16.7	15.0
28	0	95	5	0.28	0.21	0.18	0.09	17.4	12	16.6	15.0
29	2	90	8	0.6	0.425	0.21	0.083	19.4	9.5	18.4	12
30	2	96	2	0.4	0.3	0.21	0.11	18.7	10.5	17.8	13
31	1	97	2	0.55	0.4	0.22	0.15	18.5	12	17.6	15.0
32	1	84	15	0.25	0.19	0.1	0.06	18.7	9.5	17.8	12
33	1	97	2	0.43	0.35	0.21	0.14	18.4	10.5	17.4	13
34	2	95	3	0.9	0.78	0.4	0.19	18.3	11	17.4	14
35	0	94	6	0.19	0.15	0.11	0.08	17.3	12.5	16.4	15.5
36	0	100	0	0.28	0.25	0.19	0.14	17.5	11	16.6	14
37	1	96	3	0.425	0.32	0.2	0.1	18.9	10	18.1	12.5
38	1	96	3	0.26	0.2	0.15	0.09	18.2	12.5	17.3	16
39	0	100	0	0.8	0.6	0.32	0.15	19.5	8.5	18.5	11
40	0	95	5	0.24	0.2	0.13	0.082	18.3	10	17.3	13
41	2	95	3	0.39	0.3	0.18	0.1	17.9	11	16.9	14.5
42	1	96	3	0.4	0.3	0.19	0.1	17.9	10	17.0	13
43	2	96	2	0.5	0.39	0.21	0.12	17.9	12	17.0	15.0
44	2	93	5	0.28	0.2	0.14	0.09	17.3	10	16.4	13
45	2	96	2	0.5	0.37	0.21	0.15	17.8	9.5	16.8	12
46	1	95	4	0.29	0.21	0.15	0.09	17.3	11	16.4	14.5
47	2	94	4	0.31	0.29	0.18	0.1	17.4	12	16.6	15.0
48	0	95	5	0.21	0.19	0.13	0.081	17.4	13	16.5	16.5
49	2	96	2	0.7	0.5	0.35	0.17	18.3	10.5	17.4	13.5
50	2	96	2	0.425	0.31	0.21	0.15	17.9	11	17.0	14
51	1	93	6	0.28	0.2	0.14	0.08	17.9	9.5	17.1	12
52	1	94	5	0.3	0.23	0.16	0.09	17.7	10	16.7	12.5
53	1	93	6	0.3	0.21	0.15	0.085	17.7	10	16.7	12.5
54	0	91	9	1	0.75	0.3	0.085	20.7	9	19.6	11.5
55	0	100	0	0.2	0.19	0.12	0.09	16.2	15.5	15.2	18.5
56	0	95	5	0.22	0.19	0.12	0.08	16.7	14.5	15.5	18
57	0	91	9	0.28	0.2	0.12	0.079	17.5	9.5	16.7	12
58	0	86	14	0.3	0.2	0.11	0.06	18.5	10	17.3	12
59	0	62	38	0.2	0.14	0.054	0.02	19.2	9	18.1	11.5
60	0	98	2	0.201	0.18	0.11	0.09	16.7	13	15.9	16
61	0	97	3	0.2	0.19	0.12	0.085	16.9	12	16.0	15
62	1	97	2	0.7	0.48	0.21	0.1	18.9	11	18.0	14
63	0	71	29	0.25	0.19	0.08	0.03	19.2	9.5	18.2	11.5
64	1	83	16	0.3	0.21	0.11	0.05	19.7	9	18.7	12
65	0	64	36	0.3	0.19	0.062	0.03	20.0	9	19.0	11.5
66	5	87	8	1	0.8	0.425	0.09	20.2	8.5	19.3	12
67	1	95	4	1	0.8	0.425	0.11	20.0	10.0	19.0	12.5
68	1	68	31	0.19	0.14	0.075	0.033	18.6	10.5	17.6	13
69	0	84	16	0.21	0.2	0.15	0.05	19.2	9.5	18.1	12
70	0	83	17	0.18	0.17	0.1	0.07	16.9	11.5	15.6	14.5
71	0	86	14	0.23	0.21	0.16	0.07	16.8	11	15.9	13.5
72	0	94	6	0.21	0.2	0.11	0.08	16.6	13.5	15.7	17
73	0	95	5	0.29	0.21	0.18	0.09	16.7	10.5	15.9	13.5
74	2	90	8	0.6	0.425	0.2	0.08	18.6	9	17.6	11.5
75	2	96	2	0.4	0.3	0.2	0.13	18.2	10.5	17.3	13.5
76	1	97	2	0.57	0.4	0.22	0.15	18.4	11	17.4	13.5
77	1	84	15	0.24	0.19	0.1	0.06	17.3	11.5	16.4	14.5

78	1	97	2	0.44	0.35	0.2	0.15	18.3	10.5	17.4	13
79	2	95	3	0.85	0.7	0.4	0.21	17.3	9	16.3	11
80	0	94	6	0.2	0.15	0.1	0.08	17.5	10.5	16.7	13

m: modified Proctor test, *s*: standard Proctor test

Table 3.2 Summary of Statistical values of input and output parameters

	Fines (%)	**Sand (%)**	D_{50}	C_u	***CE***	***MDD***	***OMC***
Maximum	100	46	0.8	11.765	2696	20.75	18.50
Minimum	50	0	0.09	1.375	592	15.17	8.00
Average	88.5	10.44	0.274	4.55	1644	17.62	12.19
Standard Deviation	11.63	11.48	0.166	2.51	1054.4	1.183	2.18

Table 3.3 Cross correlation between the inputs and output

	Sand (%)	**Fines (%)**	D_{50}	C_u	***CE***	***MDD***	***OMC (%)***
Sand (%)	1						
Fines (%)	-0.995	1					
D_{50}	0.40154	-0.4269	1				
C_u	-0.556	0.5448	0.324	1			
CE	0	0	0	0	1		
MDD	-0.447	0.431	0.332	0.774	0.42	1	
OMC (%)	0.309	-0.284	-0.205	-0.455	-0.643	-0.76	1

3.2 Database preprocessing

The database has been normalized between 0 to 1 for LS-SVM model by using the formula:

$$X_n = \frac{X - X_{\min}}{X_{\max} - X_{\min}}$$

For ANN and MARS modeling, the actual database has been used.

3.3 Developed model equations

3.3.1 ANN model equation

In the neural network model, Levenberg-Marquartd back-propagation has been used for minimization of error for both the models. The hyperbolic tangent sigmoid transfer function for input-hidden layer and linear transfer function for hidden layer-output layer has been used to construct the model equation which is found to be optimum for both the models.

The final ANN model equation can be given as follows:

$A_1 = -11.167\ a - 13.829\ b - 99.4175\ C_u + 0.00034\ CE + 1363.383$

$A_2 = 3.808\ a - 3.126\ b - 7.536\ C_u - 0.00003331\ CE - 328.6133$

$A_3 = 0.03571\ a + 0.0228\ b - 0.3913\ C_u - 0.000068\ CE - 1.6421$

$A_4 = 51.961\ a + 39.188\ b + 32.941\ C_u - 2.336\ CE - 1.2856$

$MDD = -0.8841 \tanh(A_1) + 0.8931 \tanh(A_2) - 4.8144 \tanh(A_3) - 0.8341 \tanh(A_4) + 20.293$ (3.2)

$A_1 = -11.2872\ a + 10.0223\ b - 2.7313\ C_u - 0.3716\ CE + 28.6707$

$A_2 = 1.2647\ a + 1.1810\ b - 2.5487\ C_u - 0.0005\ CE - 118.8911$

$A_3 = -0.0542\ a - 0.0574\ b + 0.0154\ C_u + 0.0149\ CE - 37.0904$

$A_4 = 3.2903a + 2.9314\ b - 3.6901\ C_u + 0.0005\ CE - 295.7113$

$OMC = -3.1872 \tanh(A_1) + 3.8722 \tanh(A_2) - 26.9176 \tanh(A_3) + 1.4801 \tanh(A_4) + 11.7996$ (3.3)

3.3.2 LS-SVM model equation

For the LS-SVM model, Radial basis kernel function has been used for transformation of the inputs in the prediction of MDD and OMC. The optimum values of bias, regularization parameter and with of radial basis function is given below and the values for Lagrange multiplier for all the inputs have been represented in Figure 3.1 and 3.2:

For prediction of *MDD*

γ	901.8988
b	1.967575
σ^2	19.42052

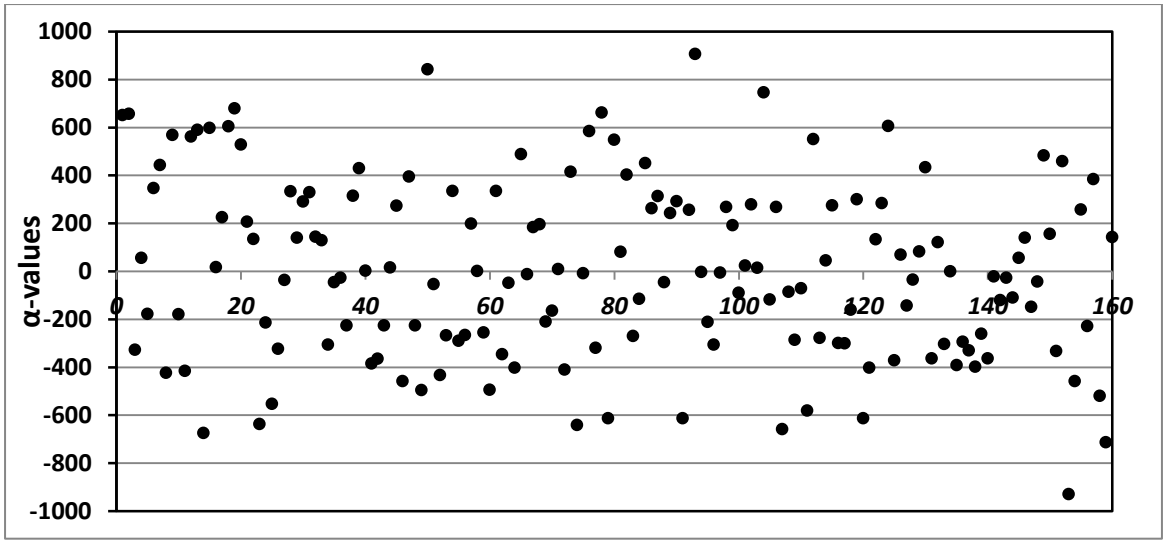

Figure 3.1 Corresponding α-values in the prediction of MDD

For prediction of *OMC*

b	21.71217
γ	117744.3
σ^2	93.74005

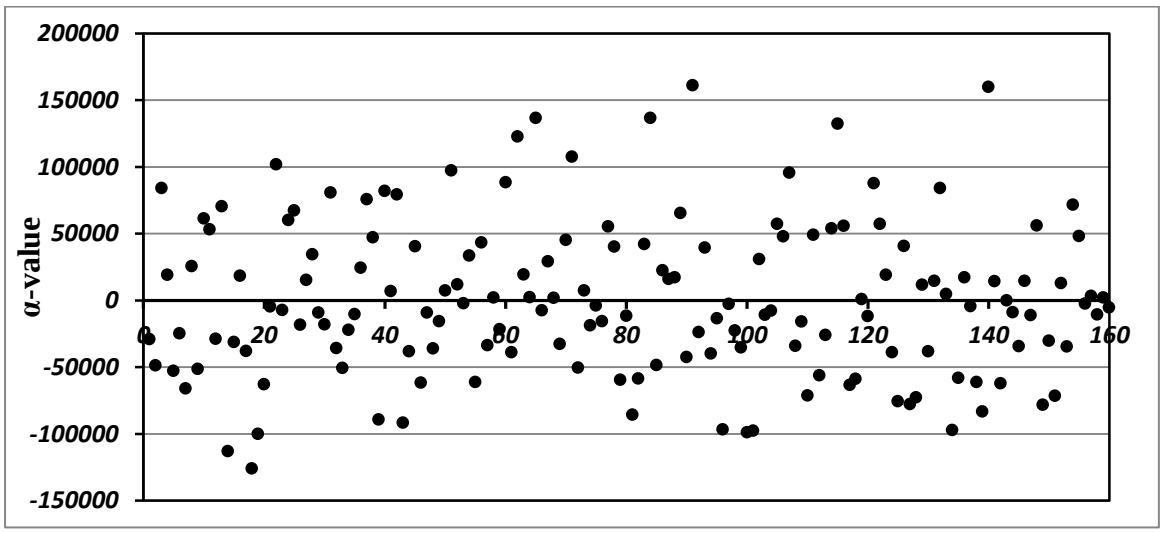

Figure 3.2 Corresponding α-values in the prediction of OMC

3.3.3 MARS model equation

For developing the MARS, 19 and 16 basis functions have been introduced in forward phase for modeling MDD & OMC respectively and in backward elimination phase, 6 and 5 basis functions have been removed from the MARS model. So, the final MARS contains 13 and 11 basis functions respectively for MDD and OMC. The optimal MARS model is given below

Table 3.4 Basis functions of MARS model

Basis Functions	*MDD*	*OMC*
$\mathbf{BF_1}$	max(0, C_u -5.33)	max(0, *CE* -592)
$\mathbf{BF_2}$	max(0, 5.33 -C_u)	max(0, C_u -3.29) × max(0, *b* -2)
$\mathbf{BF_3}$	max(0, 2700 -*CE*)	max(0, C_u -3.29) × max(0, 2 -*b*)
$\mathbf{BF_4}$	max(0, *b* -5)	BF_2 × max(0, C_u -3.53)
$\mathbf{BF_5}$	max(0, 5 -*b*)	BF_2 × max(0, 3.53 -C_u)
$\mathbf{BF_6}$	BF_5 × max(0, C_u -2.93)	max(0, C_u -3.29) × max(0, C_u -3.64)
$\mathbf{BF_7}$	BF_5 × max(0, 2.93 -C_u)	max(0, C_u -3.29) × max(0, 3.64 -C_u)
$\mathbf{BF_8}$	BF_1 × max(0, *b* -38)	max(0, 3.29 -C_u) × max(0, *b* -2)
$\mathbf{BF_9}$	BF_5 × max(0, *a* -94)	max(0, 3.29 -C_u) × max(0, 2 -*b*)
$\mathbf{BF_{10}}$	BF_5 × max(0, 94 -*a*)	max(0, 3.29 -C_u) × max(0, *a* -95)
$\mathbf{BF_{11}}$	BF_9 × max(0, 2.23 -C_u)	max(0, 3.29 -C_u) × max(0, 95 -*a*)
$\mathbf{BF_{12}}$	BF_4 × max(0, C_u -4.17)	
$\mathbf{BF_{13}}$	BF_4 × max(0, 4.17 -C_u)	

$$MDD = 18.2 + 0.438\ BF_1 - 0.377\ BF_2 - 0.000473\ BF_3 + 0.0327\ BF_4 + 0.19\ BF_5 - 0.0857\ BF_6 - 0.766\ BF_7 + 0.0411\ BF_8 + 0.0461\ BF_9 + 0.603\ BF_{10} + 0.173\ BF_{11} - 0.00906\ BF_{12} - 0.0478\ BF_{13} \quad (3.4)$$

$$OMC = 13.6 - 0.00131\ BF_1 - 0.0203\ BF_2 - 0.516\ BF_3 + 0.00271\ BF_4 + 21.7\ BF_5 - 0.0304\ BF_6 - 41.2\ BF_7 + 0.743\ BF_8 - 1.37\ BF_9 + 0.592\ BF_{10} - 0.858\ BF_{11} \quad (3.5)$$

Then all the models for the prediction of Maximum Dry density (MDD) were compared as per Root Mean Square Error (RMSE) and Mean Absolute Percentage Error (MAPE).

3.4 Performance comparison among all the models

The error criteria like MAE, MAPE, RMSE, R and R^2 for all the models in the prediction of *MDD* and *OMC* are presented in Table 3.5 and 3.6 respectively. The results of MARS have been compared with ANN and LS-SVM model developed. The comparisons have been done in terms of Mean Absolute Percentage Error (MAPE), and Root Mean Square Error (RMSE). Figure 3.7 and 3.8 depict the bar chart of MAPE and RMSE for training dataset, respectively. It is observed from Figure 3.7 and 3.8 that the developed MARS outperform ANN and LS-SVM models. MARS does not give a generalizing function for the

entire dataset, but splits the whole model into linear regions and produces discrete functions for each of the produced linear area. Researches emphasized that regression equations obtained by the MARS technique make robust and coherent parameter valuations. Figure 3.5 and 3.6 represents the actual versus predicted value of *MDD* and *OMC* respectively and Figure 3.3 and 3.4 presents the performance of MARS model in the prediction of *MDD* and *OMC* respectively.

Table 3.5 Results of Different Models for Prediction of MDD of sandy soil

Model	Model Inputs			MAE	RMSE	MAPE	Correlation coefficient (R)	Coefficient of determination (R^2)
Mujtaba et al. (2013)	***C_u, CE***	**Regression**		0.432	0.512	2.46	0.9	0.81
Model I	***C_u, CE***	**ANN**	**Training**	0.436	0.52	2.48	0.9	0.81
			Testing	0.4	0.49	2.31	0.9	0.81
		SVM	**Training**	0.41	0.494	2.35	0.911	0.829
			Testing	0.45	0.54	2.526	0.89	0.767
		MARS	**Training**	0.35	0.43	2	0.936	0.875
			Testing	0.353	0.42	2.2	0.923	0.853
Model II	***a, b, C_u, CE***	**ANN**	**Training**	0.335	0.43	1.89	0.935	0.872
			Testing	0.35	0.43	2.04	0.926	0.858
		SVM	**Training**	0.322	0.4	1.845	0.934	0.871
			Testing	0.415	0.486	2.38	0.928	0.853
		MARS	**Training**	0.32	0.39	1.82	0.94	0.887
			Testing	0.33	0.4	1.91	0.937	0.877
Model III	***a, b, D_{50}, C_u, CE***	**ANN**	**Training**	0.35	0.44	2	0.935	0.87
			Testing	0.39	0.47	2.24	0.92	0.815
		SVM	**Training**	0.36	0.45	2.06	0.92	0.848
			Testing	0.369	0.462	2.11	0.93	0.86
		MARS	**Training**	0.314	0.4	1.79	0.93	0.877
			Testing	0.3	0.41	1.72	0.94	0.89

***a* : Sand (%), *b* : Fines (%)**

Table 3.6 Results of Different Models for Prediction of OMC of sandy soil

Model	Model Inputs			MAE	RMSE	MAPE	Correlation coefficient (R)	Coefficient of determination (R^2)
Mujtaba et al. (2013)	***C_u, CE***	**Regression**		0.963	1.21	7.85	0.83	0.69
Model I	***C_u, CE***	**ANN**	**Training**	0.91	1.18	7.62	0.855	0.71
			Testing	1.05	1.2	8.9	0.857	0.687
		SVM	**Training**	0.94	1.17	7.72	0.84	0.705
			Testing	0.931	1.174	7.44	0.85	0.719
		MARS	**Training**	0.81	0.98	6.75	0.89	0.79
			Testing	0.756	0.93	6.24	0.91	0.825
Model II	***a, b, C_u, CE***	**ANN**	**Training**	0.856	1.08	6.93	0.874	0.76
			Testing	0.851	1.05	7.18	0.871	0.745
		SVM	**Training**	0.865	1.09	7.06	0.867	0.751
			Testing	0.91	1.12	7.606	0.855	0.72
		MARS	**Training**	0.74	0.94	6.17	0.903	0.815
			Testing	0.72	0.95	5.97	0.896	0.8
Model III	***a, b, D_{50}, C_u, CE***	**ANN**	**Training**	0.845	1.05	6.92	0.88	0.77
			Testing	0.82	1.01	6.93	0.879	0.764
		SVM	**Training**	0.83	1.08	6.71	0.87	0.758
			Testing	0.859	1.05	7.11	0.868	0.753
		MARS	**Training**	0.75	0.934	6.15	0.907	0.822
			Testing	0.77	0.93	6.52	0.9	0.8

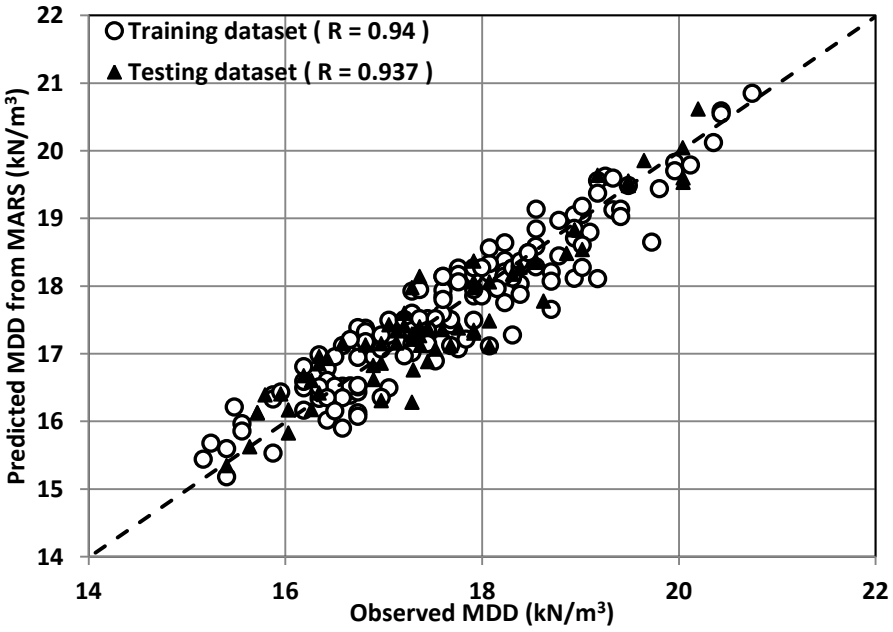

Figure 3.3 Performances of MARS model for prediction of MDD

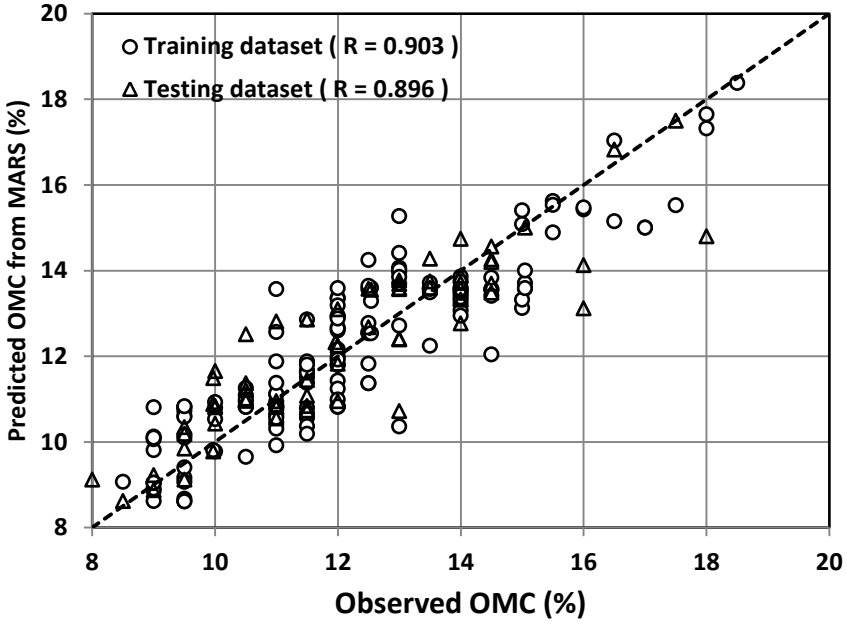

Figure 3.4 Performances of MARS model for prediction of OMC

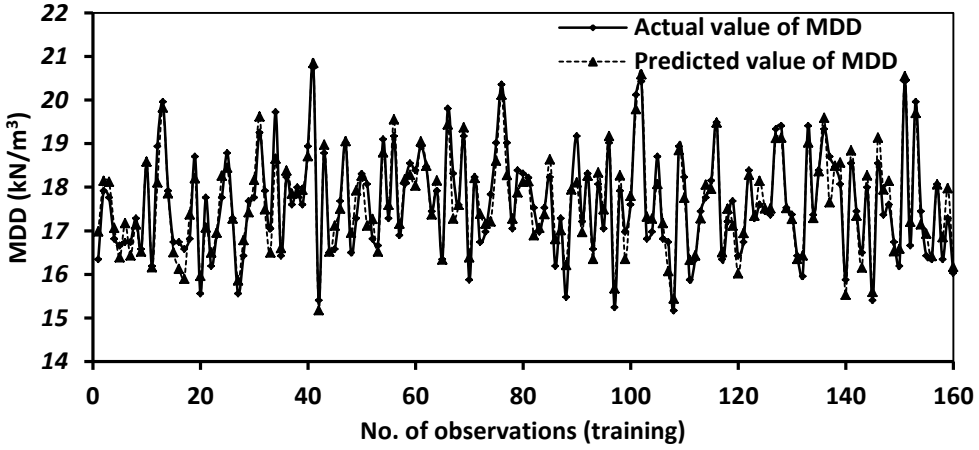

Figure 3.5 Comparison between actual and predicted value of MDD using MARS

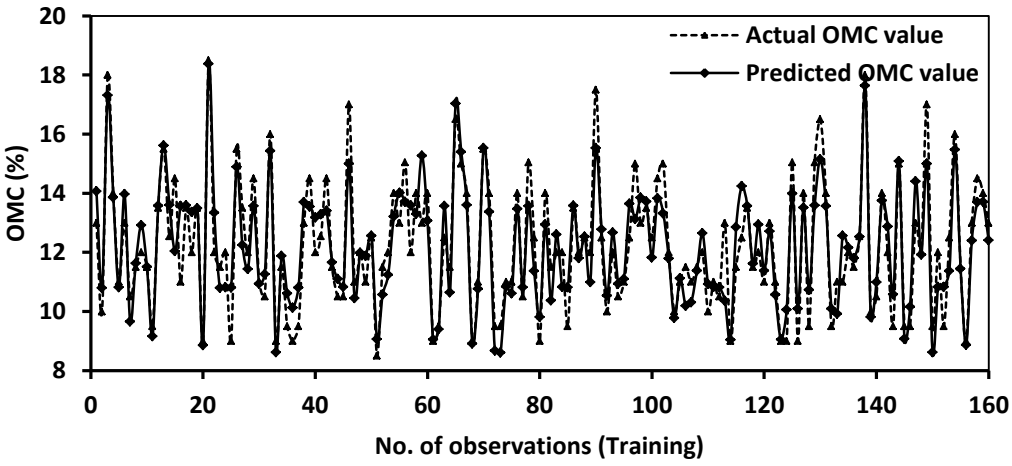

Figure 3.6 Comparison between actual and predicted value of OMC using MARS

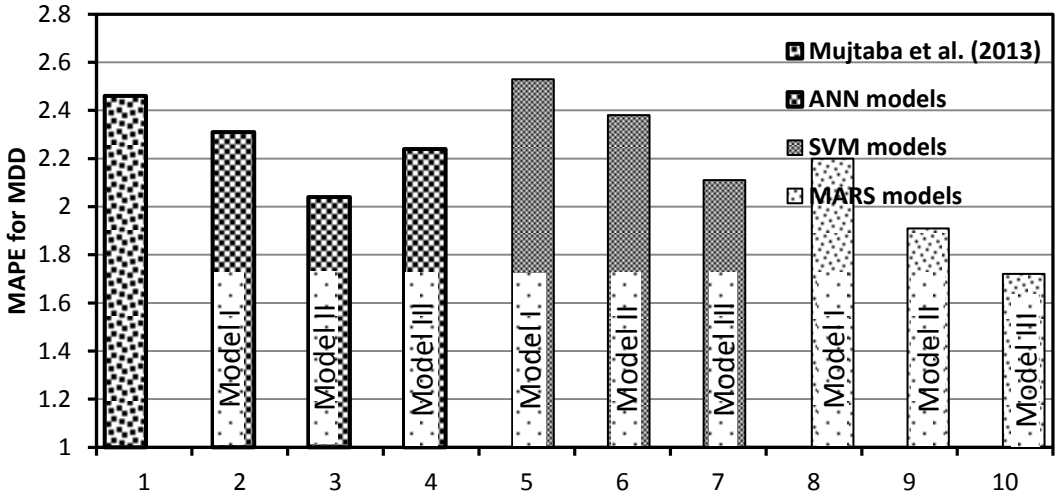

(a)

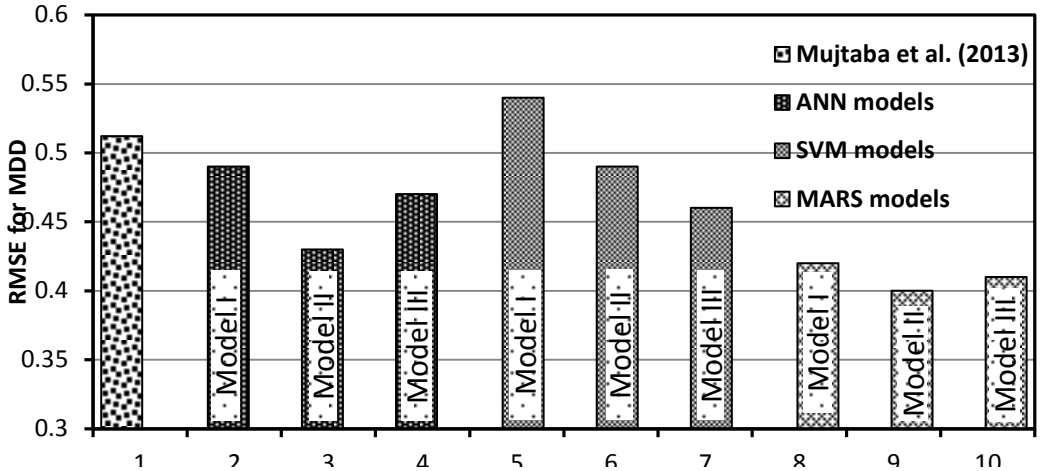

(b)

Figure 3.7 Comparison between different models in terms of (a) MAPE and (b) RMSE for the prediction of MDD.

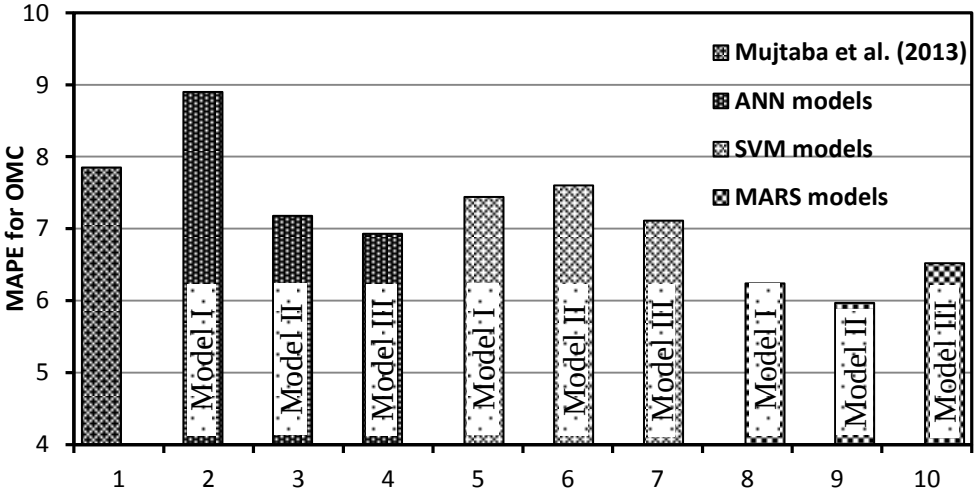

(a)

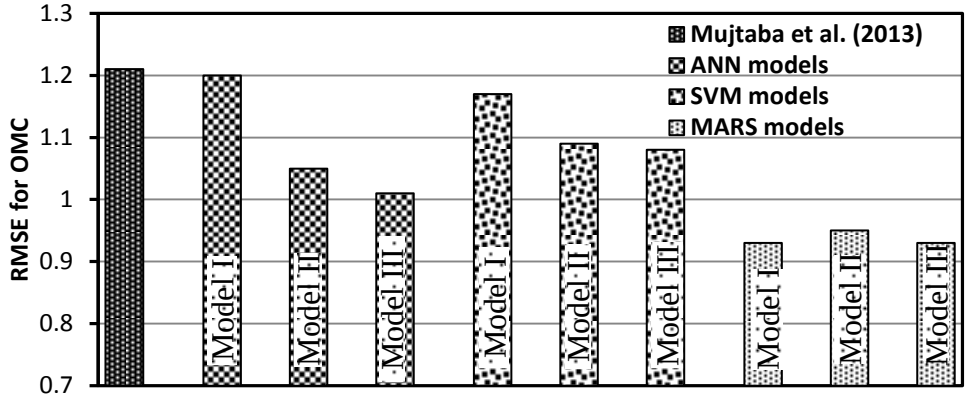

(b)

Figure 3.8 Comparison of different models in terms of (a) MAPE and (b) RMSE for the prediction of OMC

It is seen that model II and III gives better correlation as reflected by higher R^2 values for both *MDD* and *OMC* as compared to model I. When compared in terms of over fitting ratio (i.e. ratio of RMSE for testing and training data), the value of over fitting ratio of model II is very closer to 1. Model II has an advantage of having 4 inputs. The basis functions of model are presented in Table 3.5.The MARS model equations for the prediction of *MDD* and *OMC* are given by Equations 10 & 11.

3.5 Sensitivity Analysis

Iman and Hora (1990) have investigated the performance of a sensitivity measure based on the percentage variance in *f* explained by any input variable X_i. This technique is known as measure of importance, and its use is associated with the estimation of the quantity

$$S_i = \frac{Var_{xi}[E(f|X_i)]}{Var(f)} \tag{3.6}$$

where $E(f|X_i)$ indicates the expectation value of *f* when the i^{th} variable is fixed to the value X_i , $Var_{xi}[.]$stands for the variance of the argument over all the possible values of X_i and Var(*f*) is the unconditional (total) variance of *f*. In the present paper, the outcomes in the *f* are observed by keeping mean of the X_i value fixed for other arguments varying. From the sensitivity analysis, it is found that the value of sand and fines are more sensitive towards the

evaluation of *MDD* (i.e. 89% and 5% respectively) and *OMC* (25% and 57% respectively) followed by C_u and compaction energy. The sensitivity of all the input variables is presented in Figure 3.9. Hence for the prediction, the values of sand (%) and fines (%) have to be determined very precisely in the laboratory.

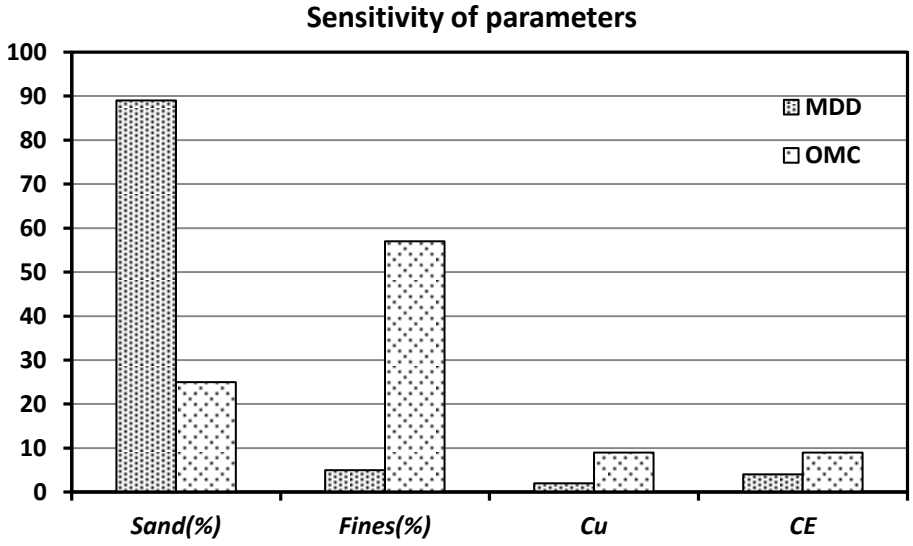

Figure 3.9 Sensitivity of the parameters in prediction of MDD and OMC

3.6 Discussion

The performances of the developed models are better than other models and gives very promising result in prediction. In the present study, model equations has been developed and compared with the regression model given by Mujtaba et al. (2013). Based on the developed MARS model, the following conclusion may be drawn:

1. MARS gives a simplified equation for prediction of *MDD* and *OMC*.
2. The predictability of MARS equation is found to be better than the empirical equations.
3. Based on sensitivity analysis, it is observed that sand (%) affects *MDD* and both sand and fines (%) affects *OMC*.

CHAPTER 4
PREDICTION OF RELATIVE DENSITY OF CLEAN SAND

4.1 Introduction

Field compaction of sands usually involves different equipments with the compaction energy varying significantly. The relative density is the better indicator for specifying the compaction of granular soil. If the relative density can be correlated simply by any index property of the granular soil, it can be more useful in the field. The relative density is defined in terms of voids ratio and the minimum and maximum voids ratio depend on the mean grain size. Therefore, the effect of mean grain size (D_{50}) on the relative density of sand has been studied at different compaction energies (E). Relative density of sand is greatly affected by particle shapes, sizes and their packing.

Several publications have appeared in recent years documenting the prediction of compaction parameters of coarse-grained soils (Korfiatis and Manikopoulos 1982; Omar et al. 2003). Very limited researches have been done to predict the relative density of sand. Present work is an attempt to develop a single empirical correlation for relative density of clean sands. In this paper a model is developed to predict the relative density using LS-SVM which proves to be very effective. The empirical correlation given by Patra et al. (2010) is given by

$$D_r = A\, D_{50}^{-B} \tag{4.1}$$

where A and B are the functions of compaction energy. A = 0.216 ln E – 0.85 and B = – 0.03 ln E + 0.306.

4.2 Selection of the input parameters

The maximum, minimum, average, and standard deviation for the data set used for modeling are shown in Table 4.1. The successful application of a method depends upon the identification of suitable input parameters. The selection of the input parameters is based on

the correlation coefficient (R) with output. This is shown in Table 4.2. The more the absolute value of correlation coefficient is close to value 1, the stronger will be the linear correlation while closer to 0 will be very poor correlation between the tested variables. From Table 4.2, it is observed that G_s, C_u, D_{50} and E are the important input parameters for predicting D_r having cross-correlation values of 0.232, -0.188, -0.196 and 0.846 respectively. Out of these variables, two parameters D_{50} and E are considered for development of model for direct comparison with the regression model reported by Patra et al. (2010). The training dataset has been reported in Table 4.3.

Table 4.3 statistical values of parameters

	G_s	C_u	D_{50}	E	D_r
Mean	2.633	3.606	0.880	1240	65.7
Standard Deviation	0.061	2.233	0.614	913	18.1
Minimum	2.535	1.420	0.340	360	33.7
Maximum	2.764	9.830	2.600	2700	97.7

Table 4.4 cross-correlation between different parameters

	G_s	Cu	D_{50}	E	D_r
G_s	1.000				
Cu	-0.718	1.000			
D_{50}	-0.682	0.895	1.000		
E	0.000	0.000	0.000	1.000	
D_r	0.232	-0.188	-0.196	0.846	1.000

4.3 Database preprocessing

The database has been normalized between 0 to 1 for LS-SVM model by using the formula:

$$X_n = \frac{X - X_{\min}}{X_{\max} - X_{\min}}$$

For ANN and MARS modeling, the actual database has been used.

Table 4.3 Training database considered for the model development

Sl. No.	G_s	C_u	D_{50}	E	D_r	α-values
1	2.662	1.88	0.39	360	42.76	-15.05
2	2.726	1.44	0.35	600	67.88	-5.86
3	2.668	1.61	0.35	360	43.4	-30.37
4	2.634	1.82	0.54	360	42.81	29.96
5	2.662	1.88	0.39	2700	95.16	64.19
6	2.564	4.39	1.1	600	54.22	-22.54
7	2.556	3.93	0.8	360	35.97	-0.67
8	2.705	1.57	0.35	2700	94.53	17.76
9	2.726	1.44	0.35	2700	87.3	-106.97
10	2.581	4.55	1	600	54.57	-17.66
11	2.717	2.09	0.55	2700	80.61	-85.23
12	2.702	1.77	0.36	360	45.85	21.55
13	2.692	1.74	0.36	1300	82.01	16.25
14	2.586	7.27	1.95	2700	81.96	16.56
15	2.702	1.77	0.36	600	69.67	38.58
16	2.652	1.94	0.58	2700	80.01	-82.80
17	2.556	3.93	0.8	2700	77.88	-38.84
18	2.556	4.68	1.25	2700	78.65	-25.07
19	2.652	1.94	0.58	600	64.16	38.70
20	2.697	1.53	0.41	360	41.97	-37.25
21	2.656	1.65	0.36	1300	83.83	45.68
22	2.663	1.77	0.36	360	41.22	-55.67
23	2.764	1.54	0.375	2700	89.09	-58.06
24	2.564	4.39	1.1	2700	77.08	-43.94
25	2.696	1.74	0.35	600	68.83	19.36
26	2.578	9.83	2.4	2700	84.19	2.06
27	2.554	4	1.25	1300	69.02	10.00
28	2.649	2.05	0.35	360	42.79	-18.98
29	2.566	4.38	1.2	1300	71.26	25.83
30	2.627	2.29	0.7	1300	72.97	2.63
31	2.589	7.33	1.7	600	58.22	8.20
32	2.655	2.13	0.58	2700	88.32	58.68
33	2.554	4	1.25	600	53.3	-26.48
34	2.717	2.09	0.55	600	58.9	-57.67
35	2.711	1.67	0.38	2700	91.45	-11.39
36	2.566	4.38	1.2	360	38.55	45.03
37	2.688	2.26	0.6	360	37.34	-31.20

38	2.711	1.67	0.38	1300	80.42	-2.96
39	2.592	7.41	1.6	360	37.43	8.57
40	2.575	3.27	0.49	2700	87.2	39.14
41	2.59	6.67	1.1	1300	75.32	14.18
42	2.729	1.44	0.365	600	69.82	33.23
43	2.589	7.33	1.7	2700	80.88	-11.69
44	2.729	1.44	0.365	2700	94.73	26.69
45	2.697	2.05	0.35	1300	82.11	19.47
46	2.574	4.39	1.25	2700	78.29	-20.52
47	2.684	2.05	0.38	600	66.69	8.40
48	2.697	1.53	0.41	600	63.23	-54.61
49	2.586	7.27	1.95	1300	73.5	-3.48
50	2.576	4.44	0.78	600	54.66	-16.34
51	2.535	3.8	1.3	2700	76.54	-23.30
52	2.574	5	1.1	1300	76.52	83.90
53	2.702	1.77	0.36	1300	74.07	-115.79
54	2.662	1.88	0.39	600	63.34	-50.83
55	2.584	8.08	1.4	600	59.96	6.57
56	2.711	1.67	0.38	600	65.59	-24.61
57	2.707	1.61	0.34	360	46.17	12.38
58	2.59	4.55	0.93	1300	68.44	-40.51
59	2.649	2.05	0.35	600	63.75	-51.64
60	2.668	1.61	0.35	600	63.92	-67.08
61	2.576	4.44	0.78	360	36.1	0.53
62	2.668	1.61	0.35	2700	96.45	51.18
63	2.663	1.77	0.36	1300	79.39	-27.07
64	2.556	3.93	0.8	1300	69.5	-25.66
65	2.679	1.8	0.35	600	65.86	-27.83
66	2.584	7.37	2.4	1300	73.63	11.90
67	2.655	2.13	0.58	600	63.82	36.01
68	2.554	4	1.25	360	34.31	-15.62
69	2.649	2.05	0.35	2700	89.46	-46.50
70	2.574	5	1.1	600	61.26	90.84
71	2.584	7.37	2.4	360	36.27	11.38
72	2.696	1.74	0.35	360	45.14	4.93
73	2.679	1.8	0.35	360	43.42	-20.82
74	2.576	4.44	0.78	1300	69.59	-30.43
75	2.601	3	0.41	360	39.76	-9.04
76	2.589	6.67	2.6	2700	81.67	-0.36
77	2.592	7.41	1.6	1300	73.16	-21.56
78	2.566	4.38	1.2	2700	86.09	108.90
79	2.592	7.41	1.6	2700	80.63	-22.21

80	2.764	1.54	0.375	1300	78.33	-40.68
81	2.726	1.42	0.75	2700	79.84	0.00
82	2.581	4.24	1	600	53.14	-41.74
83	2.652	1.94	0.58	1300	74.83	-13.47
84	2.652	1.94	0.58	360	41.58	24.94
85	2.584	7.37	2.4	2700	82.97	17.12
86	2.607	4.86	1.4	1300	71.52	9.71
87	2.589	6.67	2.6	360	36.48	-4.96
88	2.617	7.69	1.15	360	36.9	-11.93
89	2.578	9.83	2.4	1300	71.23	1.73
90	2.627	2.29	0.7	360	41.03	54.77
91	2.656	1.65	0.36	360	44.48	-7.03
92	2.537	3.66	1.3	360	34.49	-1.94
93	2.586	7.27	1.95	360	34.94	-15.77
94	2.729	1.44	0.365	1300	80.76	-4.44
95	2.587	7.37	2.4	2700	81	-15.73
96	2.587	7.37	2.4	600	56.15	-16.62
97	2.7	1.85	0.34	2700	95.34	36.21
98	2.662	1.88	0.39	1300	83.03	47.18
99	2.584	7.37	2.4	600	58.36	20.24
100	2.59	4.55	0.93	2700	77.64	-43.29
101	2.581	4.55	1	1300	71.28	10.47
102	2.697	2.05	0.35	600	69.91	51.10
103	2.607	4.86	1.4	2700	77.86	-41.76
104	2.627	2.29	0.7	600	62.49	56.43
105	2.564	4.39	1.1	1300	68.75	-21.03
106	2.711	1.67	0.38	360	43.57	-14.51
107	2.592	7.41	1.6	600	57.53	-9.63
108	2.688	2.26	0.6	600	60.57	-8.75
109	2.68	1.57	0.35	2700	96.78	55.28
110	2.535	3.8	1.3	1300	66.58	-16.76
111	2.566	4.38	1.2	600	59.56	68.29
112	2.617	7.69	1.15	2700	84.36	10.56
113	2.589	6.67	2.6	1300	71.54	-6.45
114	2.693	1.65	0.35	600	69.94	34.65
115	2.663	1.77	0.36	2700	91.75	-14.95
116	2.627	2.29	0.7	2700	85.61	67.05
117	2.697	2.05	0.35	2700	94.37	35.39
118	2.764	1.54	0.375	600	68.93	25.26
119	2.693	1.65	0.35	1300	81.88	9.14
120	2.584	8.08	1.4	2700	82.83	1.55
121	2.696	1.74	0.35	2700	94.4	21.93

122	2.729	1.44	0.365	360	46.66	21.24
123	2.68	1.57	0.35	360	48.66	55.43
124	2.601	3	0.41	2700	85.27	-35.31
125	2.586	7.27	1.95	600	56.36	-9.90
126	2.656	1.65	0.36	600	66.78	-13.84
127	2.693	1.65	0.35	2700	93.4	1.77
128	2.578	9.83	2.4	360	35.19	-1.39
129	2.655	2.13	0.58	1300	77.56	34.00
130	2.7	1.85	0.34	600	69.67	33.85
131	2.684	2.05	0.38	1300	81.85	26.77
132	2.68	1.57	0.35	1300	83.86	41.58
133	2.556	4.68	1.25	1300	68.57	-32.33
134	2.574	5	1.1	2700	87.3	107.98
135	2.634	1.82	0.54	600	64.39	25.15
136	2.557	5.56	1.25	2700	81.13	-9.86
137	2.668	1.61	0.35	1300	82.43	17.99
138	2.707	1.61	0.34	2700	97.72	66.04
139	2.554	4	1.25	2700	80.28	28.38
140	2.726	1.42	0.75	600	54.63	-45.71
141	2.684	2.05	0.38	360	44.2	13.78
142	2.557	5.56	1.25	600	54.26	-36.35
143	2.726	1.42	0.75	360	36.15	-29.39
144	2.581	4.55	1	360	34.9	-18.90
145	2.679	1.8	0.35	1300	83.33	35.08
146	2.556	4.68	1.25	600	54.53	-19.98
147	2.575	3.27	0.49	600	59.18	-17.12
148	2.535	3.8	1.3	360	34.43	-7.07
149	2.697	2.05	0.35	360	46.98	50.90
150	2.59	6.67	1.1	360	38.66	17.79
151	2.589	6.67	2.6	600	58.29	0.70
152	2.702	1.77	0.36	2700	88.47	-69.65
153	2.726	1.44	0.35	1300	77.94	-57.56
154	2.574	4.39	1.25	600	55.91	8.23
155	2.68	1.57	0.35	600	70.3	38.08
156	2.59	4.55	0.93	360	35	-17.10
157	2.764	1.54	0.375	360	45.73	13.83
158	2.576	4.44	0.78	2700	79.15	-22.98
159	2.697	1.53	0.41	1300	79.77	-2.41
160	2.717	2.09	0.55	360	38.72	-26.42

4.4 Different developed model equations

The different model equations developed from ANN, SVM and MARS are presented in the next segments.

4.4.1 ANN Model equation

In the neural network model, Levenberg-Marquartd back-propagation has been used for minimization of error. The hyperbolic tangent sigmoid transfer function for input-hidden layer and linear transfer function for hidden layer-output layer has been used to construct the model equation. The final ANN model equation can be given as follows:

$A_1 = 0.02581\ C_u - 0.0149\ D_{50} - 0.0052\ E + 2.5603$

$A_2 = -\ 0.1201\ C_u + 0.0784\ D_{50} - 0.0005664\ E + 1.608$

$A_3 = -\ 9.4862\ C_u + 1.7756\ D_{50} - 0.000566\ E + 24.5579$

$A_4 = 0.1203\ C_u + 3.5595\ D_{50} - 0.0002435\ E - 1.0608$

$$D_r = 69.4104 - 18.4647 \tanh(A_1) - 12.1131 \tanh(A_2) + 1.4698 \tanh(A_3) - 11.4156 \tanh(A_4) \quad (4.2)$$

4.4.2 LS-SVM Model equation

For the LS-SVM model, Radial basis kernel function has been used for transformation of the inputs. The optimum values of bias, regularization parameter and with of radial basis function is given below and the values for Lagrange multiplier for all the inputs has been represented in Figure 4.1:

$b = -0.0896,\ \gamma = 299.0974,\ \sigma^2 = 3.2817$

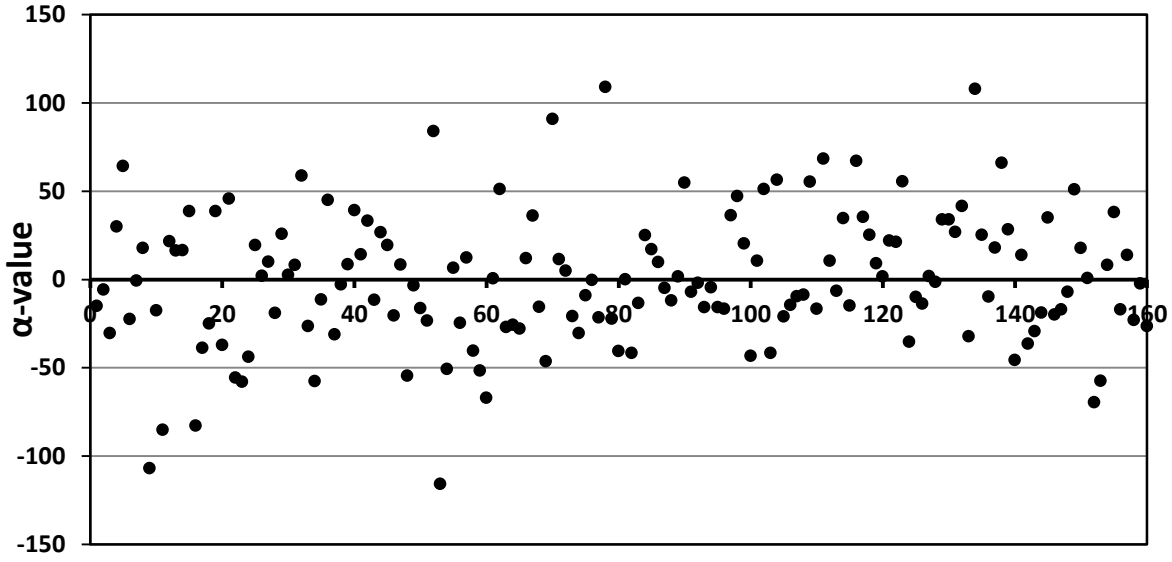

Figure 4.1 Corresponding α-value for the LS-SVM model for prediction of D_r

4.4.3 MARS model equation

For developing the MARS, 13 basis functions have been introduced in forward phase and in backward elimination phase, 4 basis functions have been removed from the MARS model. So, the final MARS contains 9 basis functions. The optimal MARS model is given below

$$BF_1 = \max(0, E - 600)$$

$$BF_2 = \max(0, 600 - E)$$

$$BF_3 = \max(0, 0.75 - D_{50})$$

$$BF_4 = BF1 \times \max(0, 2700 - E)$$

$$BF_5 = \max(0, 3 - C_u)$$

$$BF_6 = BF_1 \times \max(0, 0.41 - D_{50})$$

$$BF_7 = BF_5 \times \max(0, C_u - 2.26)$$

$$BF_8 = BF_5 \times \max(0, 2.26 - C_u)$$

$$BF_9 = \max(0, 5 - C_u)$$

$$D_r = 58.1 + 0.0114 \times BF_1 - 0.0887 \times BF_2 + 26.7 \times BF_3 + 6.14e\text{-}006 \times BF_4 + 7.83 \times BF_5 + 0.0247 \times BF_6 + 258 \times BF_7 - 2.64 \times BF_8 - 2.98 \times BF_9 \quad (4.3)$$

4.5 Result comparison and discussion

The statistical performances i.e. Mean Absolute Error (MAE), Root Mean Squared Error (RMSE), Correlation Coefficient (R) and coefficient of efficiency (R^2) for the model are presented in Table 4.4.

Table 4.4 Results of Different Models for Prediction of Relative density of clean sand

Model	Model Inputs			RMSE	MAPE	(R)	(R^2)	Over-fitting ratio
Patra et al. (2010)	D_{50}, E	Regression		5.23	7.38	96	0.92	
Model I	D_{50}, E	ANN	Training	2.45	3.28	0.99	0.98	1.04
			Testing	2.54	3.07	0.99	0.98	
		SVM	Training	2.48	3.15	0.99	0.98	0.99
			Testing	2.46	3.18	0.99	0.98	
		MARS	Training	2.27	2.78	0.992	0.984	0.97
			Testing	2.21	2.94	0.993	0.985	
Model II	C_u,D_{50}, E	ANN	Training	2.31	2.9	0.992	0.984	0.91
			Testing	2.1	2.48	0.993	0.985	
		SVM	Training	2.27	2.68	0.992	0.984	0.88
			Testing	2	2.7	0.994	0.988	
		MARS	Training	2.21	2.64	0.992	0.985	0.96
			Testing	2.13	2.87	0.993	0.985	
Model III	G_s,C_u,D_{50}, E	ANN	Training	2.3	2.9	0.99	0.983	0.93
			Testing	2.15	2.66	0.993	0.983	
		SVM	Training	2.1	2.44	0.992	0.986	1.05
			Testing	2.2	2.9	0.993	0.986	
		MARS	Training	2.2	2.8	0.993	0.986	0.99
			Testing	2.18	2.5	0.992	0.981	

The model was compared in terms of correlation coefficient (R) and coefficient of efficiency (R^2) to access the performance of models. The value of R has been determined by using the following equation:

$$R = \frac{n(\sum y.y_p) \quad (\sum y)(\sum y_p)}{\sqrt{[n\sum y^2 \quad (\sum y)^2][n\sum y_p{}^2 \quad (\sum y_p)^2]}}$$

where y = observed value, y_p = predicted value, n = number of observations

Smith (1986) suggested that the value of R lies between 0 to 1. He suggested some

guidelines for deciding the performance of the model. If $|R| \geq 0.8$: a strong correlation exists, $0.2 < |R| < 0.8$: correlation exists and $|R| \leq 0.2$: a weak correlation exists. When the value of |R| is greater than 0.9, then a very strong correlation exists between the variables. From Table 4.3, it was observed that the value of |R| is nearly equal to 0.99; hence it shows a very strong relation between inputs and outputs.

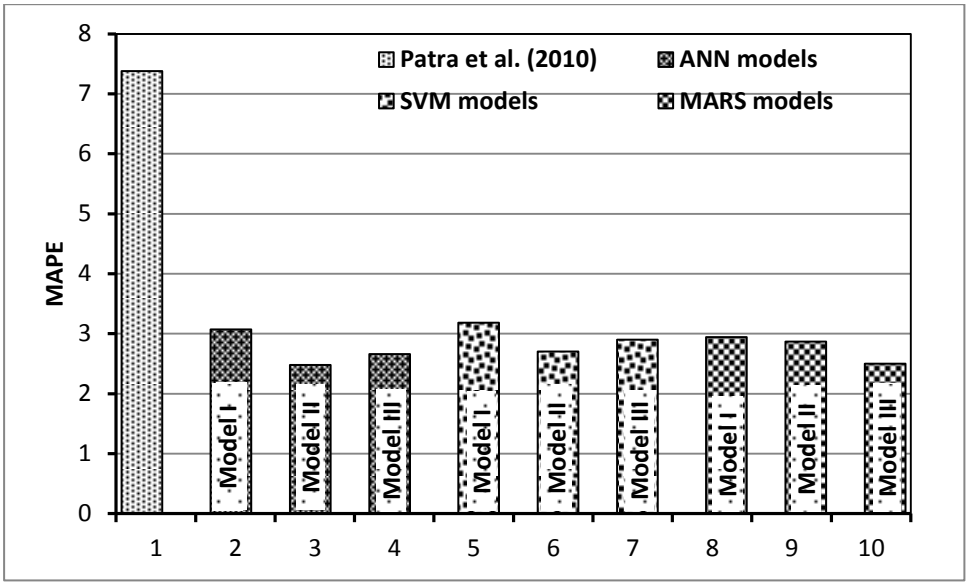

Figure 4.2 Comparison of MAPE of different models in the prediction of D_r

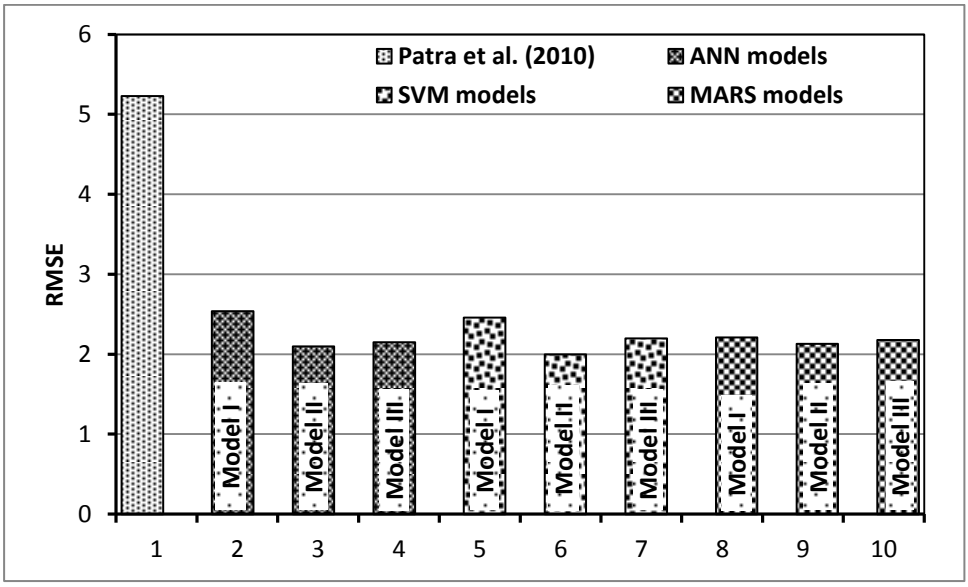

Figure 4.3 Comparison of RMSE of different models in the prediction of D_r

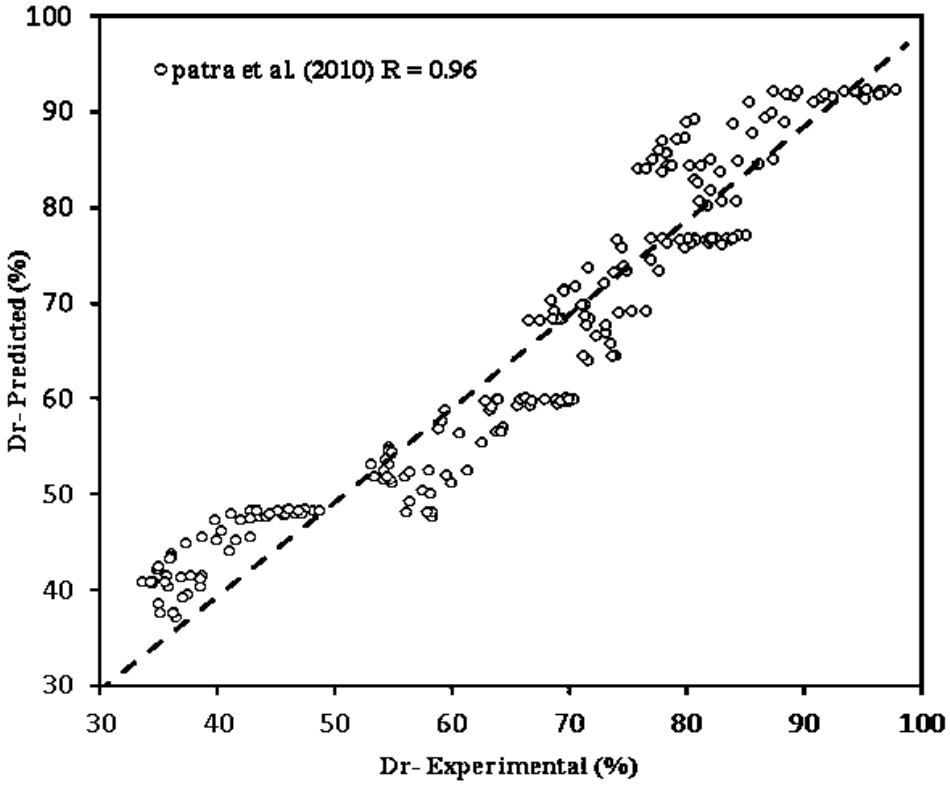

Figure 4.4 Comparison between experimental and predicted value of D_r (Patra et al., 2010).

The error criteria MAPE and RMSE has been shown in Figure 4.2 and 4.3 for all the models and it can be observed that the developed LS-SVM model shows good correlation in both training having three inputs which is comparatively the "better model" for the prediction of D_r as compared to other models. The optimum values of γ, σ^2 and b presented in Section 4.3.2 and the Lagrange multipliers are shown in Figure 4.1. By using these optimum values and α, the relative density can be predicted. The comparison of experimental and predicted value of D_r by regression model is shown in Figure 4.4 and the performance of the LS-SVM model in training and testing is shown in Figure 4.5 for present study. The variation of actual and the predicted value have been shown in Figure 4.6.

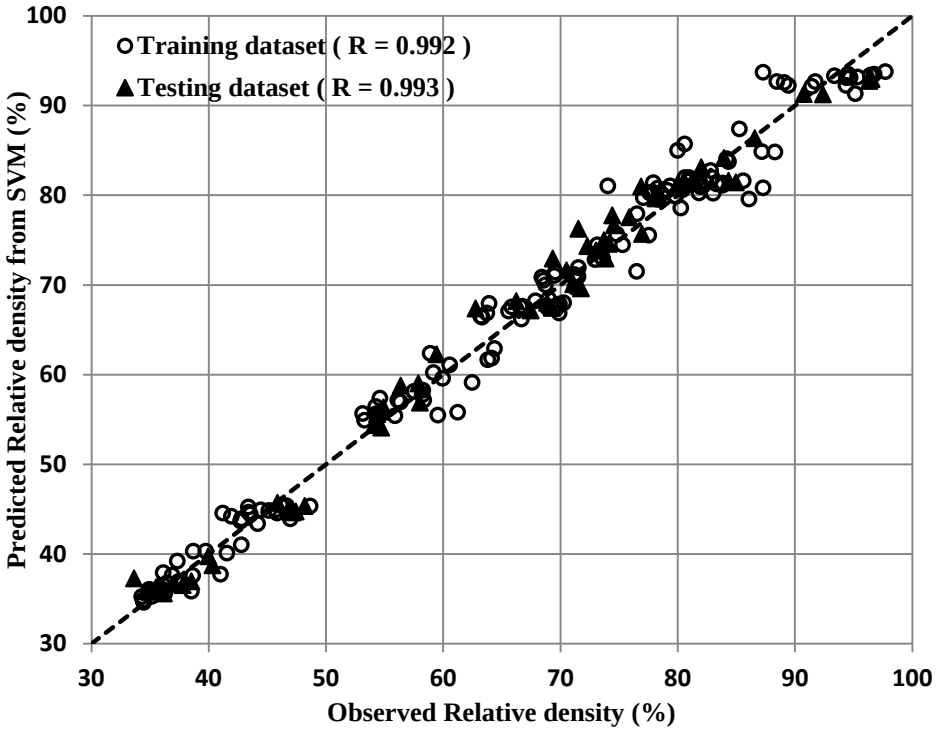

Figure 4.5 Performance of the LS-SVM model in training and testing (Present study).

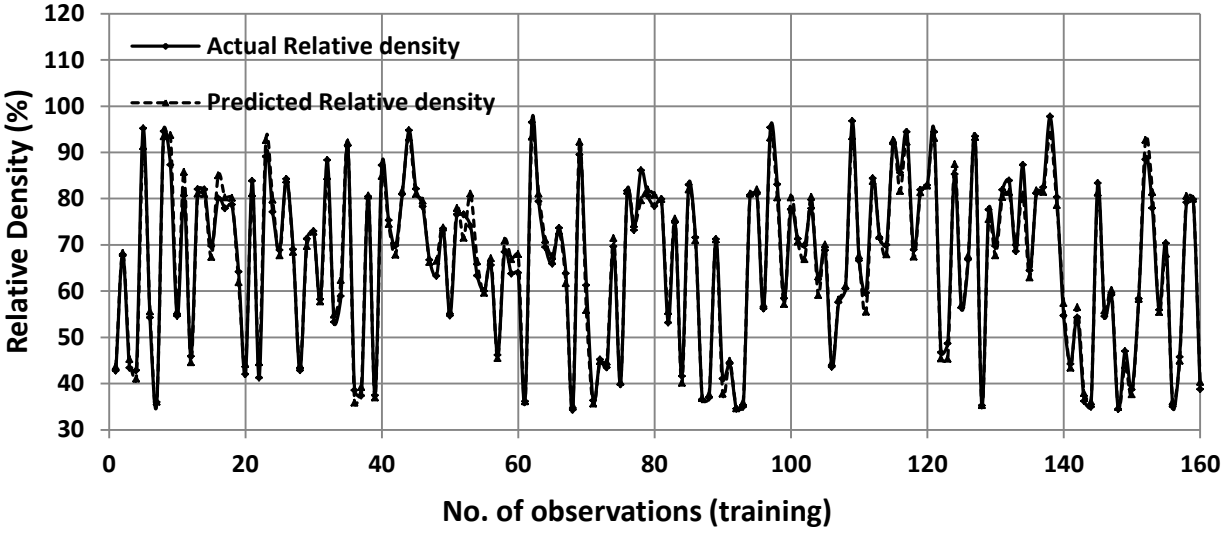

Figure 4.6 Variation of the values predicted by LS-SVM model and observed values.

4.6 Sensitivity Analysis

The details of the sensitivity analysis have been given in section 3.5.2. From the sensitivity analysis, it is found that the mean grain size of the C_u (50%) is more sensitive towards the evaluation of Relative density compared to the mean grain size (42%),

compaction energy (8%). Hence for the prediction, the value of C_u and mean grain size has to be determined very precisely. The sensitivity of different parameters has been shown in Figure 4.7.

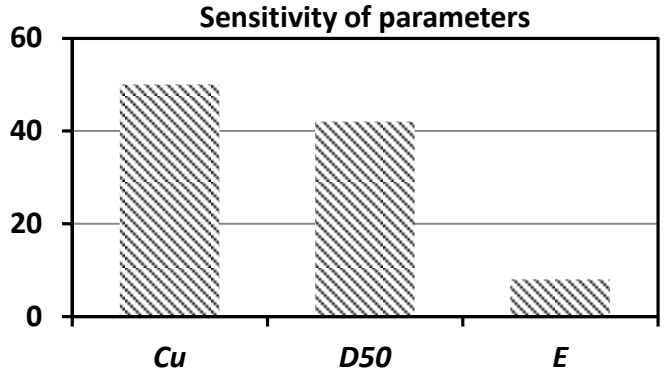

Figure 4.7 Sensitivity of the parameters

4.7 Discussion

This study presents an efficient approach for the prediction of relative density using ANN LS-SVM and MARS. The proposed SVM model has shown good agreement with experimental results as corresponding correlation coefficients were found to be 0.99. The proposed model is valid for the ranges of the experimental database used for the modeling. To obtain the main effects of each variable on relative density, sensitivity analysis has been performed. As a result, coefficient of uniformity and mean diameter of the sand particles affect the model significantly. The proposed model and formulation for relative density is quite accurate and hence practically applicable in the field.

CHAPTER 5
PREDICTION OF COMPRESSION INDEX OF CLAY

5.1 Introduction

Settlement due to expulsion of pore water is of engineering importance. Due to increase in stress caused by the construction of foundations or other loads, the soil compresses. The various causes of compression are deformation of soil particles, relocation of soil particles, and expulsion of water or air from the void spaces. To calculate settlement in clayey soil layers, laboratory consolidation tests which depict one-dimensional compression behavior need to be performed on samples taken as representative.

As the oedometer test in laboratory takes a much longer time than simpler index property tests various attempts have been made to estimate this index to obtain an initial estimate and also to cross check the results of the consolidation test. Empirical formulas relating various parameters to the compression index have been presented by many researchers (Azzouz et al., 1976; Koppula, 1981; Herrero, 1980; Park and Lee, 2011; Nishida, 1956; Cozzolino, 1961; Sower, 1970; Ahadiyan et al., 2008; Al-Khafaji and Andersland, 1992; Yoon and Kim, 2006; Ozer et al., 2008). However, due to fact that the index is affected by multiple parameters and highly non-linear, simple regression analysis is not sufficient and hence non-linear regression such as ANN, SVM and MARS are more effective. The advantage of these techniques is the ability of learning complex relationships between multi-dimensional data and has been applied in a number of geotechnical problems where mathematical models sustain simplifications, lack of robustness or are not available at all.

The data set (Kalantary, 2012) consists of consolidation test data for soil samples collected from 125 construction sites in province of Mazandaran, Iran. Different models have been developed using this set of data. The results from the developed model have been

compared with the results obtained by using various empirical equations available in literature. It is found that the ANN model gives better prediction and finally the model equation is presented.

5.2 Data base selection

In the current paper, 391 experimental results of compression index have been used. The data set is subdivided into two groups as training data set (290 data) and testing data set (101 data). Liquid Limit (LL), Plasticity index (PI), natural water content (w_n) and initial void ratio (e_0) are considered as input and compression index (C_c) as output parameter. From the cross-correlation matrix (Table 5.1), it is observed that the above inputs w_n and e_0 with cross-correlation values of 0.75 and 0.82 respectively affect C_c more than the other input parameters (i.e. LL and PI). Hence three models (considering two inputs, three inputs and four inputs as shown in Table 5.3) are selected for the prediction of compression index. The statistical values of all the input and output parameters are given in Table 5.2.

Table 5.1 cross-correlation matrix for all data

	LL	***PI***	w_n	e_0	C_c
LL	1.00				
PI	0.97	1.00			
w_n	0.33	0.28	1.00		
e_0	0.31	0.26	0.90	1.00	
C_c	0.40	0.36	0.75	0.82	1

Table 5.2 statistical value of the parameters

	LL	***PI***	w_n	e_0	C_c
Mean	39.8	18.58	28.61	0.767	0.206
Standard Deviation	9.89	8.57	7.79	0.176	0.0774
Minimum	24	3	10.2	0.357	0.05
Maximum	81	50	70	1.882	0.628

5.3 Database preprocessing

The database has been normalized between 0 to 1 for LS-SVM model by using the formula:

$$X_n = \frac{X - X_{\min}}{X_{\max} - X_{\min}}$$

For ANN and MARS modeling, the actual database has been used.

Table 5.3 Database considered for modeling for training.

Sl. No.	*LL*	*PI*	w_n	e_0	C_c	*α*-values	Sl. No.	*LL*	*PI*	w_n	e_0	C_c	*α*-values
1	31	12	24.5	0.748	0.266	48.19	151	44	22	28.8	0.75	0.209	5.83
2	44	21	14.5	0.476	0.126	0.96	152	56	36	20.2	0.498	0.169	19.04
3	42	21	20.5	0.601	0.229	48.48	153	32	12	21.6	0.665	0.166	-0.41
4	34	13	20.5	0.565	0.076	-37.75	154	47	24	37.5	0.915	0.29	18.36
5	29	7	29.3	0.795	0.186	-5.10	155	44	23	10.2	0.357	0.08	-23.58
6	35	16	25.6	0.803	0.203	-13.18	156	58	36	34	0.867	0.196	-47.69
7	29	8	20.5	0.717	0.146	-21.72	157	29	11	24.7	0.71	0.19	8.13
8	43	21	17.2	0.73	0.206	-7.17	158	32	12	17.7	0.74	0.159	-31.45
9	41	20	35.3	0.909	0.226	-18.01	159	35	13	30.8	0.825	0.2	-8.06
10	31	10	12.7	0.63	0.236	40.86	160	52	28	17.6	0.615	0.21	31.81
11	62	34	36.5	0.959	0.375	43.02	161	34	16	27.6	0.738	0.189	-3.19
12	31	12	26.1	0.778	0.189	-8.89	162	46	25	23.8	0.647	0.123	-32.44
13	33	16	34	0.894	0.329	55.46	163	43	22	31.1	0.964	0.365	51.02
14	43	20	28.1	0.719	0.156	-18.12	164	53	35	23.1	0.642	0.169	-8.04
15	37	21	16.6	0.507	0.226	53.92	165	36	16	31.8	0.831	0.206	-9.89
16	52	28	28.9	0.806	0.28	33.59	166	36	20	20	0.562	0.163	6.28
17	41	18	27.1	0.666	0.116	-29.36	167	39	20	32.1	0.823	0.236	6.54
18	31	12	23.9	0.621	0.156	5.86	168	34	13	18.7	0.711	0.22	17.73
19	35	13	35.3	0.841	0.256	27.58	169	28	5	30.8	0.751	0.173	-2.21
20	40	21	30.9	0.926	0.379	70.88	170	45	21	23.4	0.697	0.176	-3.92
21	30	8	23.9	0.605	0.133	0.40	171	52	29	70	1.882	0.54	1.21
22	37	15	30.8	0.784	0.199	0.02	172	43	21	22.1	0.643	0.203	24.19
23	51	25	19.2	0.586	0.186	27.75	173	28	7	22.8	0.619	0.153	9.43
24	31	11	25.3	0.723	0.169	-6.89	174	49	25	39.6	0.891	0.26	2.41
25	39	21	25.3	0.647	0.259	58.58	175	29	11	29.7	0.778	0.196	-0.90
26	34	12	19.5	0.609	0.189	27.19	176	34	12	28.1	0.824	0.269	36.67
27	40	18	40.7	1.045	0.259	-21.46	177	33	9	29.5	0.784	0.143	-30.96
28	26	6	24.8	0.704	0.226	41.06	178	27	9	20	0.63	0.193	26.24
29	46	25	30.3	0.775	0.173	-28.37	179	40	18	25.2	0.588	0.16	16.21
30	52	28	19.5	0.517	0.14	7.17	180	29	7	31.4	0.839	0.15	-39.57

31	62	34	37.2	0.937	0.345	27.61
32	34	13	27.2	0.759	0.163	-19.71
33	34	13	22	0.675	0.216	30.61
34	67	43	39.1	0.939	0.36	30.08
35	35	15	36.6	0.883	0.246	7.84
36	53	28	22.4	0.583	0.169	16.50
37	37	15	33	0.88	0.209	-16.80
38	62	44	38.4	1.014	0.326	-4.13
39	39	21	21.6	0.552	0.11	-22.06
40	42	20	25.2	0.645	0.159	-0.69
41	33	8	27.2	0.881	0.266	26.02
42	46	24	33.6	0.847	0.296	38.12
43	36	19	27.2	0.678	0.153	-16.91
44	43	24	29.8	0.789	0.22	-2.39
45	32	11	20.4	0.699	0.173	-4.21
46	37	16	23.5	0.596	0.05	-60.57
47	62	36	34.4	0.806	0.312	43.79
48	29	9	26.1	0.786	0.209	7.52
49	49	29	32.1	0.805	0.233	-1.23
50	37	17	28.3	0.734	0.159	-20.19
51	31	12	22.9	0.628	0.143	-5.69
52	45	22	11.5	0.537	0.13	-16.00
53	35	13	23.2	0.652	0.206	32.81
54	35	16	25.2	0.663	0.14	-17.94
55	40	19	20	0.605	0.196	26.18
56	34	10	42.1	1.013	0.355	53.34
57	34	14	22.1	0.573	0.123	-7.93
58	41	20	21.3	0.699	0.14	-35.28
59	46	24	26.2	0.666	0.126	-31.01
60	25	5	48.7	1.222	0.41	24.47
61	47	29	31.4	0.826	0.179	-44.72
62	29	9	28.4	0.777	0.14	-34.82
63	45	26	34.5	0.808	0.319	59.15
64	39	17	41.1	0.993	0.259	-8.31
65	46	23	18.5	0.611	0.173	7.75
66	37	15	29.6	0.761	0.173	-12.26
67	29	9	25.5	0.643	0.126	-14.02
68	29	8	24.7	0.763	0.259	47.18
69	36	16	22.5	0.599	0.149	1.81
70	36	13	25.9	0.762	0.103	-60.26
71	29	11	25.1	0.658	0.149	-6.27
72	34	12	21.6	0.83	0.28	32.83

181	37	16	27.6	0.748	0.236	28.75
182	44	24	21.9	0.686	0.166	-17.55
183	53	28	23	0.608	0.16	5.27
184	48	28	32.4	0.85	0.249	-1.39
185	39	20	28.5	0.653	0.186	14.30
186	36	14	27.4	0.777	0.229	19.33
187	44	24	27	0.629	0.166	2.61
188	25	5	22.5	0.595	0.183	34.81
189	43	25	25.1	0.708	0.156	-30.11
190	32	11	28.8	0.703	0.206	26.58
191	36	17	28.8	0.759	0.21	6.48
192	29	8	26.7	0.663	0.12	-20.25
193	34	14	24.6	0.676	0.226	38.62
194	58	33	36.2	0.894	0.32	27.09
195	53	27	39.8	0.97	0.252	-29.34
196	30	11	26.1	0.752	0.183	-4.82
197	30	8	20.3	0.546	0.149	19.36
198	36	17	26.5	0.676	0.159	-8.19
199	50	29	31.2	0.74	0.259	33.68
200	36	14	33.7	0.844	0.203	-9.88
201	43	19	29.8	0.828	0.186	-24.93
202	39	21	21.6	0.552	0.11	-22.06
203	44	26	32.1	0.761	0.199	-10.71
204	40	21	23.7	0.585	0.22	47.70
205	27	8	25.3	0.661	0.156	1.73
206	42	20	30.3	0.755	0.193	-2.40
207	41	24	16.4	0.605	0.173	-5.29
208	34	13	42.2	1.161	0.219	-67.95
209	34	12	25.2	0.675	0.229	45.88
210	52	31	45.7	1.132	0.379	10.71
211	45	22	27.1	0.809	0.22	-4.65
212	34	12	24.1	0.668	0.106	-35.58
213	45	22	27.1	0.652	0.18	12.61
214	33	12	28	0.703	0.103	-43.34
215	49	28	34.4	0.864	0.223	-21.23
216	53	29	39	0.98	0.26	-29.57
217	28	9	19.5	0.73	0.113	-50.62
218	57	34	35	0.88	0.256	-11.04
219	51	32	32	0.829	0.31	40.25
220	56	35	25.2	0.569	0.146	-6.84
221	44	24	37.8	0.965	0.229	-34.74
222	35	15	23.5	0.507	0.11	-1.01

73	42	19	40.3	1.04	0.27	-14.86
74	38	19	35.4	0.859	0.249	10.19
75	45	22	19.7	0.661	0.149	-19.36
76	30	10	31.1	0.874	0.209	-12.49
77	33	10	22.6	0.632	0.116	-19.19
78	52	31	19.9	0.582	0.166	6.46
79	38	17	21.8	0.563	0.103	-20.69
80	27	5	11.1	0.519	0.126	-6.52
81	27	8	22.4	1	0.196	-51.57
82	31	11	29.8	0.831	0.176	-25.67
83	36	15	28.9	0.711	0.216	27.78
84	42	21	47.6	1.135	0.37	32.20
85	55	27	25.3	0.719	0.209	14.85
86	31	11	27.2	0.769	0.176	-12.02
87	32	14	24.4	0.824	0.276	30.60
88	32	11	29.7	0.822	0.213	1.88
89	40	19	26.7	0.669	0.133	-22.94
90	57	34	39.2	1.091	0.302	-39.42
91	39	16	25.1	0.672	0.13	-22.06
92	56	28	36.9	0.909	0.27	-3.39
93	36	14	27.7	0.677	0.136	-15.67
94	31	11	38.2	0.967	0.266	3.39
95	36	12	21.3	0.502	0.11	4.27
96	43	20	26.9	0.732	0.163	-18.41
97	61	37	23.2	0.586	0.159	4.34
98	39	19	30.1	1.012	0.4	64.20
99	47	25	28.9	1.137	0.402	20.12
100	34	14	24.6	0.676	0.225	37.95
101	58	35	39	1.059	0.385	22.53
102	33	10	31.4	0.768	0.252	44.88
103	49	28	36.5	0.97	0.29	-3.87
104	29	10	27.2	0.77	0.183	-7.03
105	49	25	20.1	0.638	0.09	-51.11
106	50	27	22.2	0.614	0.166	5.09
107	41	17	30.6	0.727	0.173	-2.22
108	34	13	22.1	0.66	0.173	6.05
109	60	32	55.7	1.357	0.5	11.65
110	57	35	32.7	0.904	0.282	1.88
111	54	30	31.2	0.776	0.183	-24.87
112	24	3	10.6	0.368	0.09	-9.12
113	54	31	29.8	0.755	0.149	-42.91
114	50	26	33.5	0.827	0.296	41.43

223	31	11	41.5	1.195	0.259	-47.66
224	31	7	27.5	0.738	0.173	0.82
225	30	10	54.3	0.943	0.282	-8.88
226	81	50	37.8	0.966	0.27	-17.03
227	54	31	29.8	0.755	0.149	-42.91
228	79	45	57.4	1.587	0.628	2.90
229	32	8	39.4	0.979	0.266	2.58
230	40	20	32.5	0.793	0.186	-17.42
231	29	7	22.7	0.637	0.183	26.03
232	36	17	26.5	0.676	0.159	-8.19
233	40	19	19.4	0.528	0.149	12.50
234	58	35	27.3	0.807	0.229	-1.45
235	39	19	28.5	0.725	0.183	-3.90
236	39	17	25.8	0.73	0.196	4.67
237	60	30	26.3	0.733	0.196	2.59
238	37	15	27.6	0.873	0.329	58.20
239	39	17	31.9	0.837	0.2	-14.83
240	46	25	30.3	0.775	0.173	-28.37
241	49	28	32.8	0.797	0.309	53.48
242	47	26	29.8	0.785	0.173	-32.54
243	29	9	25	0.691	0.149	-10.29
244	27	7	28.5	0.735	0.173	-1.20
245	40	19	19	0.715	0.219	9.25
246	46	24	26.2	0.666	0.126	-31.01
247	46	22	13.6	0.407	0.113	3.50
248	37	16	25.1	0.738	0.203	6.10
249	29	10	30.1	0.75	0.223	25.73
250	56	34	36.1	0.983	0.306	-5.70
251	32	14	29.5	0.744	0.173	-11.15
252	57	33	22.4	0.697	0.143	-28.13
253	44	25	34.2	0.816	0.239	5.23
254	31	10	46.4	1.232	0.465	78.27
255	47	22	20.5	0.742	0.196	-7.26
256	41	17	28.6	0.702	0.146	-15.21
257	62	36	32.7	1.054	0.355	9.24
258	32	14	30.8	0.813	0.272	38.31
259	31	15	24.4	0.711	0.159	-20.81
260	25	5	30.8	0.869	0.2	-12.59
261	36	15	33.7	0.835	0.166	-34.02
262	30	11	25.2	0.681	0.163	-1.44
263	36	15	18.5	0.567	0.106	-23.61
264	43	22	46.6	1.127	0.269	-35.41

115	39	17	36.2	0.881	0.252	11.78
116	49	24	39.1	0.948	0.32	29.78
117	33	12	36.5	0.934	0.213	-23.71
118	25	9	21	0.643	0.103	-36.30
119	33	12	28	0.703	0.103	-43.34
120	37	17	26	0.723	0.21	13.84
121	34	13	28.3	0.778	0.133	-43.51
122	36	15	25	0.697	0.183	5.01
123	36	15	56.9	1.442	0.405	0.60
124	30	10	31.1	0.856	0.25	19.16
125	42	22	21.7	0.658	0.22	27.01
126	30	10	22.6	0.602	0.13	-5.66
127	37	16	31.2	0.87	0.209	-18.06
128	31	14	26.4	0.619	0.14	-6.20
129	48	25	25.6	0.724	0.163	-21.95
130	48	25	29.9	0.756	0.163	-28.03
131	33	12	25.9	0.8	0.266	37.74
132	58	35	28.3	0.692	0.159	-21.95
133	37	16	31.8	0.776	0.166	-21.09
134	40	19	29	0.8	0.279	41.09
135	36	14	29.7	0.753	0.2	8.96
136	30	8	23.9	0.605	0.133	0.40
137	48	25	25.6	0.724	0.163	-21.95
138	43	22	29	0.798	0.209	-8.58
139	58	32	22.4	0.685	0.153	-16.20
140	40	19	37	0.923	0.309	36.61
141	32	11	20.5	0.557	0.106	-14.31
142	34	14	31.2	0.871	0.176	-38.41
143	33	13	33.6	0.789	0.279	53.32
144	59	36	27.1	0.693	0.259	45.98
145	24	4	26.3	0.695	0.169	6.97
146	29	8	26.5	0.637	0.166	16.15
147	34	12	25.8	0.692	0.173	4.96
148	27	7	26.6	0.766	0.149	-24.68
149	40	18	28.2	0.757	0.169	-18.80
150	47	27	29.8	0.736	0.25	29.72

265	27	6	37.1	0.951	0.25	-3.11
266	26	8	28.9	0.824	0.199	-6.51
267	46	22	28.6	0.801	0.153	-44.07
268	42	24	24.3	0.809	0.199	-30.69
269	54	30	31.2	0.776	0.183	-24.87
270	36	17	47.6	1.237	0.299	-28.66
271	36	17	28.8	0.759	0.206	3.82
272	68	46	34.4	0.909	0.226	-30.52
273	31	11	23.1	0.635	0.146	-3.05
274	39	19	29	0.77	0.279	48.33
275	42	20	26.9	0.716	0.216	20.09
276	56	36	28.8	0.793	0.246	9.14
277	33	10	27.8	0.707	0.176	7.75
278	35	15	27.9	0.745	0.153	-25.24
279	35	15	27.7	0.73	0.159	-17.50
280	37	14	27.1	0.72	0.176	0.18
281	27	17	21.3	0.547	0.103	-32.63
282	30	10	29.7	0.718	0.11	-40.93
283	51	27	34.8	0.854	0.249	1.20
284	40	17	39.3	0.931	0.209	-27.23
285	55	30	37.4	0.921	0.246	-25.45
286	39	21	25.3	0.647	0.259	58.58
287	42	20	44.4	1.148	0.26	-43.56
288	41	22	30.2	0.777	0.219	3.02
289	40	20	28.7	0.755	0.249	30.92
290	32	11	31	0.786	0.216	13.68

5.4 Different developed model equations

The different model equations developed from ANN, SVM and MARS are presented in the following sections.

5.4.1 ANN Model equation

In the neural network model, Levenberg-Marquartd back-propagation has been used for minimization of error. The log-sigmoid transfer function for input-hidden layer and linear transfer function for hidden-output layer has been used to construct the model equation. The final ANN model equation can be given as follows:

$A_1 = 0.5543\ LL - 0.6398\ PI + 0.1297\ w_n + 2.0933\ e_0 - 21.9155$

$A_2 = 0.3221\ LL - 0.4918\ PI - 0.3425\ w_n - 7.4531\ e_0 + 13.146$

$A_3 = 0.0012\ LL + 0.0021\ PI - 0.0156\ w_n + 1.6466\ e_0 + 0.7929$

$A_4 = -6.8441\ LL - 6.6654\ PI + 6.0927\ w_n + 3.026\ e_0 - 5.6638$

$$C_c = -0.9998 + \frac{0.2037}{1+e^{-A_1}} - \frac{0.0618}{1+e^{-A_2}} + \frac{1.4749}{1+e^{-A_3}} + \frac{0.0881}{1+e^{-A_4}} \quad (5.1)$$

5.4.2 LS-SVM Model equation

For the LS-SVM model, Radial basis kernel function has been used for transformation of the inputs. The optimum values of bias, regularization parameter and width of radial basis function is given below and the values for Lagrange multiplier (α) for all the inputs have been represented in Figure 5.1:

$b = 1.7804$, $\gamma = 51.7066$, $\sigma^2 = 17.0637$

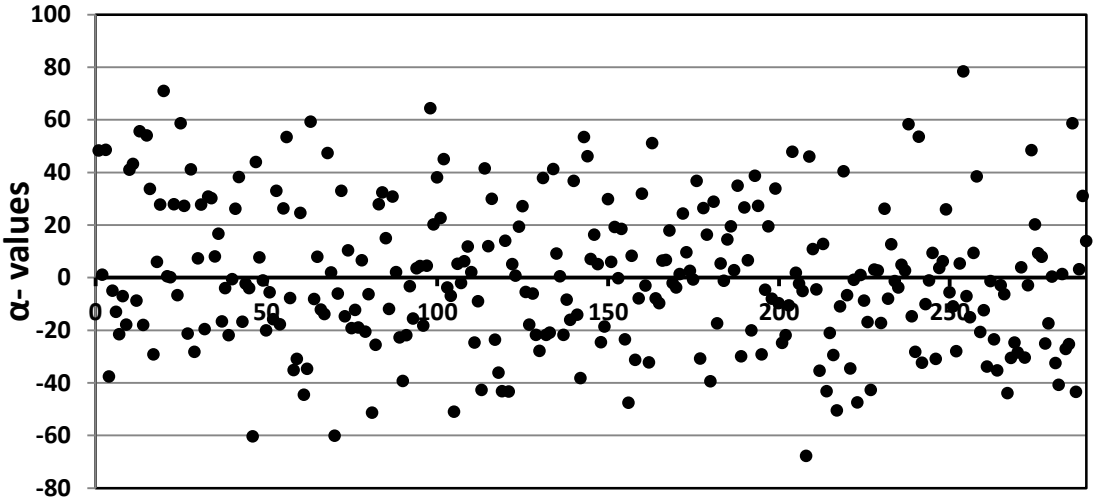

Figure 5.1 corresponding α-values in the LS-SVM model

5.4.3 MARS model equation

For developing the MARS, 11 basis functions have been presented in forward phase and in backward elimination phase, 3 basis functions have been removed from the MARS model. So, the concluding MARS model contains 8 basis functions. The best MARS model is given below

$BF_1 = \max(0, e_0 - 0.694)$

$BF_2 = \max(0, 0.694 - e_0)$

$BF_3 = BF_1 \times \max(0, PI - 13)$

$BF_4 = \max(0, e_0 - 0.694) \times \max(0, 13 - PI) \times \max(0, LL - 27)$

$BF_5 = BF_3 \times \max(0, 43 - LL)$

$BF_6 = BF_3 \times \max(0, PI - 21)$

$BF_7 = \max(0, e_0 - 0.694) \times \max(0, 13 - PI) \times \max(0, w_n - 22.4)$

$BF_8 = BF_3 \times \max(0, PI - 17)$

$$C_c = 0.174 + 0.162 \times BF_1 - 0.263 \times BF_2 - 0.0644 \times BF_3 + 0.012 \times BF_4 + 0.0178 \times BF_5 - 0.0211 \times BF_6 + 0.00141 \times BF_7 + 0.0208 \times BF_8 \quad (5.2)$$

Table 5.4 Results of Different Models for Prediction of compression index of clay

Model	Model Inputs			RMSE	MAPE	Coefficient of determination (R^2)
Model I	w_n, e_0	ANN	Training	0.042	15	0.71
			Testing	0.042	15	0.65
		SVM	Training	0.044	18	0.68
			Testing	0.043	18	0.68
		MARS	Training	0.042	17	0.7
			Testing	0.042	18	0.72
Model II	*LL*, w_n, e_0	ANN	Training	0.04	14	0.72
			Testing	0.041	15	0.73
		SVM	Training	0.042	17	0.68
			Testing	0.042	18.8	0.76
		MARS	Training	0.041	17	0.73
			Testing	0.04	16	0.68
Model III	*LL*, *PI*, w_n, e_0	ANN	Training	0.39	14	0.76
			Testing	0.04	13	0.66
		SVM	Training	0.04	17	0.72
			Testing	0.039	17	0.73

MARS	**Training**	0.0396	16.8	0.73
	Testing	0.043	17.9	0.7

5.5 Results and discussion

The models have been created and compared with the empirical correlations given by various researchers shown in Table 5.5. The comparison is made in terms of coefficient of efficiency (R^2) presented in Table 5.4 of the developed models. The performances of the empirical formulas are presented in Table 5.6. An error bar chart has been shown in Figure 5.2 for the comparison between different developed models. From the comparison it is found that model 3 of ANN and model 2 of LS-SVM are showing better performance than others. But model 3 of ANN having lower value of MAPE is the better model as compared to others. The performance of model 3 in training and testing is shown in Figure 5.3 and variation of actual and predicted values has been shown in Figure 5.4.

Table 5.5 some widely used empirical correlations

Sl. No	**Author**	**Equation**
1	Azzouz et al. (1976)	$C_c = 0.4\ (e_0 + 0.001\ w_n - 0.25\ )$
2	Azzouz et al. (1976)	$C_c = 0.01\ w_n - 0.05$
3	Koppula (1981)	$C_c = 0.01\ w_n$
4	Herrero (1980)	$C_c = 0.01\ w_n - 0.075$
5	Park and Lee (2011)	$C_c = 0.013\ w_n - 0.115$
6	Skempton (1944)	$C_c = 0.009\ (LL-10)$
7	Nishida (1956)	$C_c = 0.54\ e_0 - 0.19$
8	Cozzolino (1961)	$C_c = 0.43\ e_0 - 0.11$
9	Sower (1970)	$C_c = 0.75\ e_0 - 0.38$
10	Kalantary et al. (2012)	$C_c = 0.0074\ w_n - 0.007$
11	Kalantary et al. (2012)	$C_c = 0.3608\ e_0 - 0.0713$

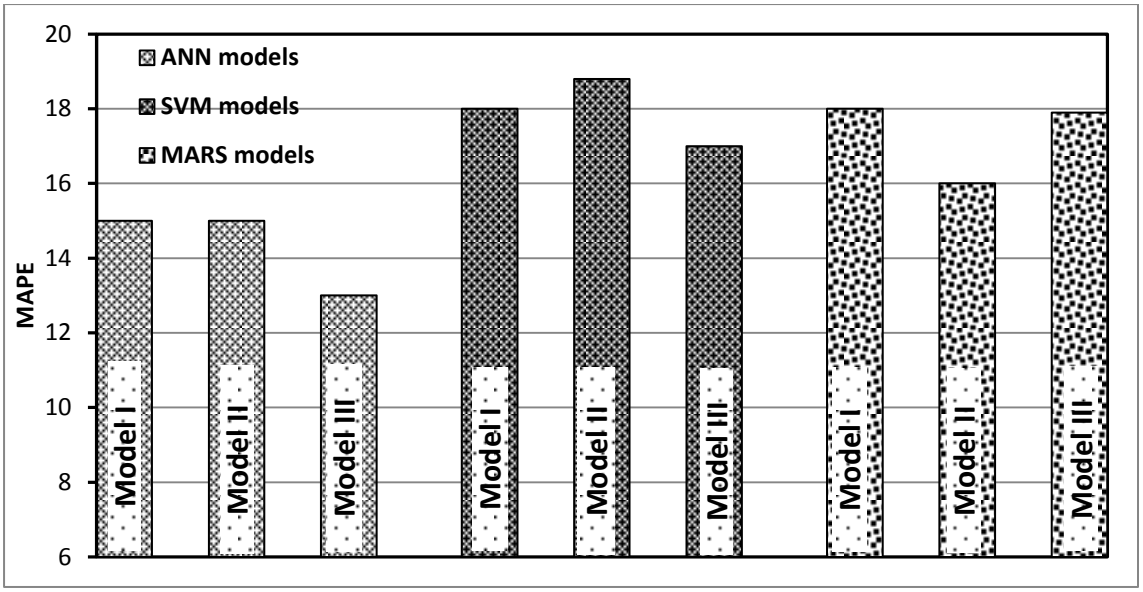

(a)

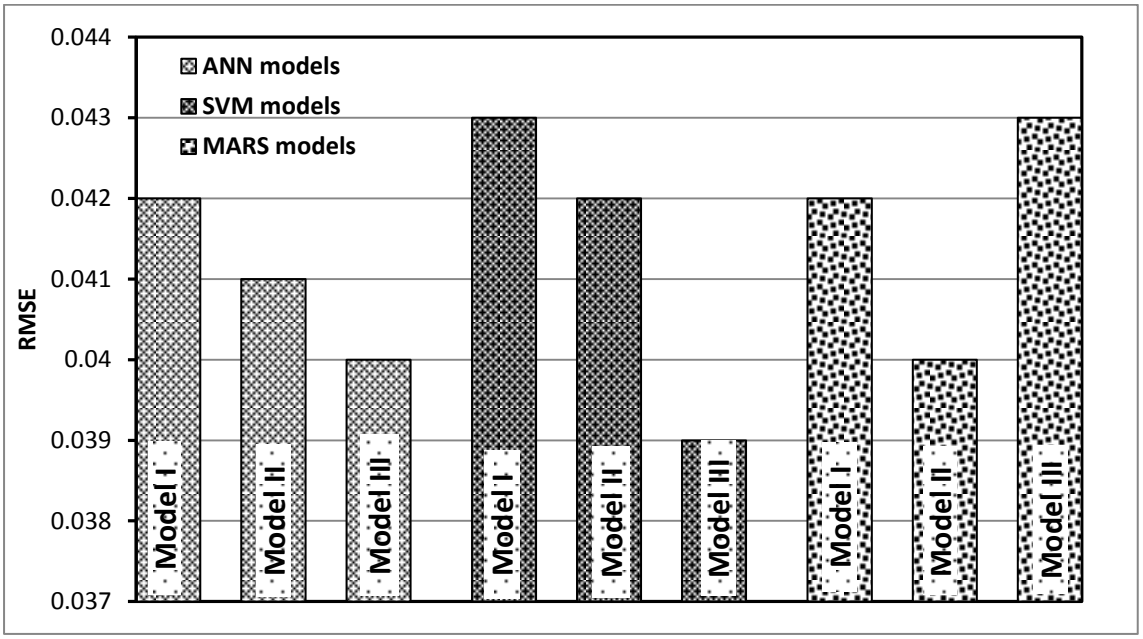

(b)

Figure 5.2 performance evaluations of different models in terms of (a) MAPE and (b) RMSE

Table 5.6 results of different models for prediction of compression index of clay

Model	Model Inputs	RMSE	R	R^2
1	e_0, w_n	0.047	0.823	0.63
2	w_n	0.063	0.75	0.56

3	w_n	0.098	0.74	0.54
4	w_n	0.055	0.75	0.49
5	w_n	0.0846	0.75	0.52
6	**LL**	0.111	0.397	0.37
7	e_0	0.057	0.82	0.67
8	e_0	0.048	0.82	0.62
9	e_0	0.082	0.82	0.615
10	w_n	0.051	0.75	0.56
11	e_0	0.044	0.823	0.677

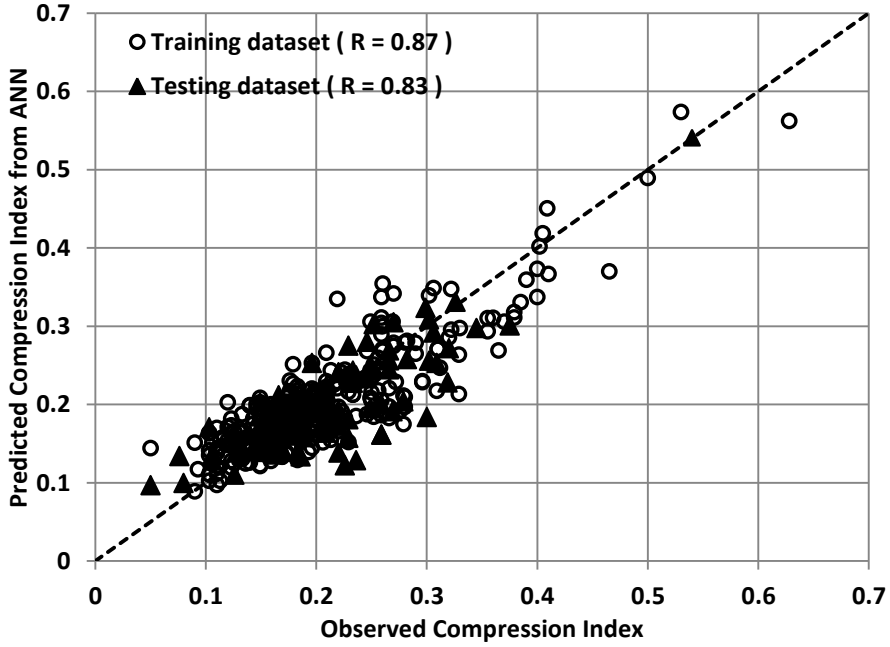

Figure 5.3 Performance of model 3 using ANN in training and testing.

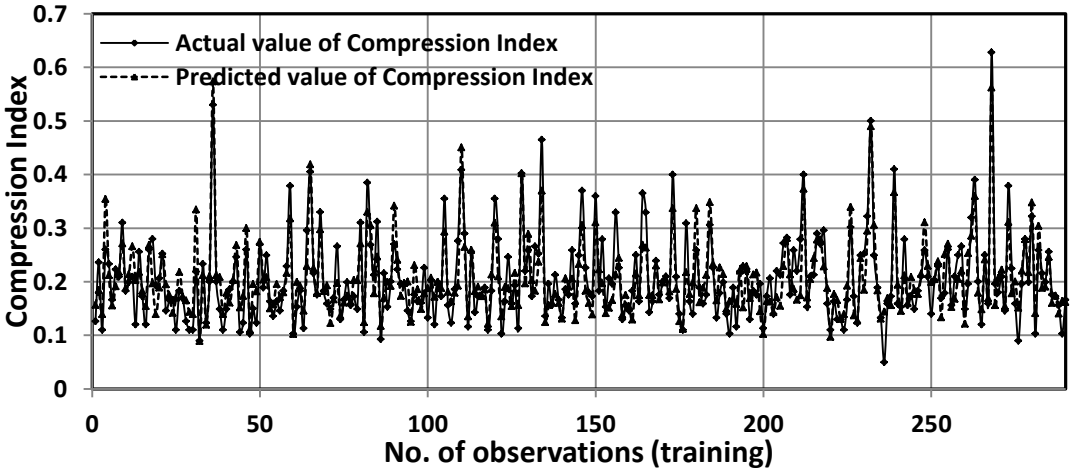

Figure 5.4 Variation of actual and predicted value from ANN of compression index

5.6 Sensitivity Analysis

Sensitivity analysis is performed for selection of important input variables. Different approaches have been suggested to select the important input variables. Goh (1994) and Shahin et al. (2002) have used Garson's algorithm (Garson, 1991) in which the input hidden and hidden output weights of trained ANN model are partitioned and the absolute values of the weights are taken to select the important input variables, and the details with example have been presented in Goh (1994). It does not provide information on the effect of input variables in terms of direct or inverse relation to the output. Olden et al. (2004) proposed a connection weight approach based on the Neural Interpretation Diagram (NID), in which the actual values of input hidden and hidden output weights are taken. It sums the products across all the hidden neurons, which is defined as S_i. The relative inputs are corresponding to absolute S_i values, where the most important input corresponds to highest S_i value. The details of connection weight approach are presented in Olden et al. (2004).

The relative importance of the four input parameters as per Garson's algorithm is presented in Table 5.7. The w_n is found to be the most important input parameter with the relative importance value being 95.85 % followed by 2.27 % for PI, 1.09 % for LL and 0.781 % for e_0. The relative importance of the present input variables, as calculated following the connection weight approach (Olden et al., 2004), is also presented in Table 5.7. w_n is found to be the most important input parameter (Si = 21.41) followed by e_0 (S_i = 0.188), LL (S_i =-0.154) and PI (S_i = 0.128). The S_i values being negative imply that LL is indirectly related and w_n, e_0 and PI are directly related to C_c value. In other words, increasing LL will lead to a reduction in the C_c and increasing w_n, e_0 and PI will increase the C_c. The sensitivity of the parameters affecting the model is presented in Figure 5.5.

Table 5.7 relative importance of different inputs as per Garson's algorithm and connection weight approach

Parameters	Garson's algorithm		Connection weight approach	
(1)	**Relative importance (%) (2)**	**Ranking of inputs as per relative importance (3)**	**S_i values as per connection weight approach (4)**	**Ranking of inputs as per relative importance (5)**
LL	1.09	3	-0.154	3
PI	2.27	2	0.128	4
e_0	0.781	4	0.188	2
w_n	95.85	1	21.41	1

where C_c = predicted value of compression index of clay from ANN.

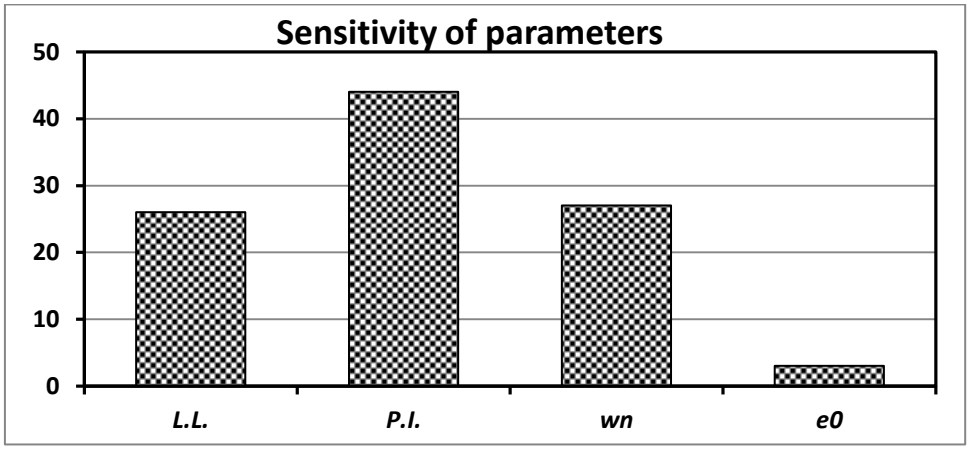

Figure 5.5 Sensitivity of different parameters

5.7 Discussions

From the present study it is observed that the developed ANN model can be used to predict compression index of clay. The results obtained with these models are compared to each other and with different regression models. The result shows that the proposed model equation gives better predictability in comparison with others. Sensitivity analysis is fulfilled to recognize the most sensitive parameters. Natural water content (w_n) is found to be the most effective parameters for prediction of compression index. From the above model equation, the compression index of clay soil can be predicted quickly and satisfactorily.

CHAPTER 6
PREDICTION OF SIDE RESISTANCE OF DRILLED SHAFT

6.1 Introduction

The two main criteria that govern the design of pile foundations are bearing capacity and settlement so that safety and serviceability requirements are attained. Drilled shafts are cast-in-situ piles installed by excavating a cylindrical volume of soil from the ground and filling the resulting void with concrete. They can range from 2 to 30 feet in diameter and can be over 300 feet in length. The installation of drilled shafts causes insignificant lateral displacement of the soil adjacent them. The calculations of shaft resistance of drilled shafts are most often performed using empirical correlations (Skempton 1959; O Neill and Reese 1999) developed on the basis of a limited number of load tests. They are particularly advantageous where huge lateral loads from extreme event limit states govern bridge foundation design. Additional applications include providing foundations for high pole lighting, communication towers. In many instances, a single drilled shaft can replace a cluster of piles eliminating the need and cost for a pile cap.

Static analysis methods are commonly used for determining the side resistance of drilled shafts. The methodologies apply the soil parameters resulting from laboratory tests to calculate the side resistance of the shafts. The most common method to evaluate the undrained side resistance is based on the total stress or alpha (α) method (Tomlinson; 1957), in which the side resistance or adhesion is related to the undrained shear strength S_u by an empirical coefficient denoted by α, the adhesion factor. This coefficient was derived mostly from field load test data on driven piles. The main criticism of the alpha method is that S_u is not a unique soil parameter and depends significantly on the type of test used, the strain rate, and the orientation of the failure plane.

The geotechnical literature has included numerous investigations and many methods,

both theoretical and experimental, to predict settlement and bearing capacity of pile foundations. However, the mechanisms of pile foundations and pile–soil interaction are ambiguous, complex, and not yet entirely understood (Reese et al. 2006; Nejad et al. 2009; Shahin 2010; Alkroosh and Nikraz 2012). Because of the uncertainties associated with the factors that affect the behavior of pile foundations, most available methods, by necessity, have been mainly based on simplifications and assumptions. This has led to limited success in terms of providing consistent and accurate predictions (Abu-Kiefa 1998; Nejad et al. 2009; Pal and Deswal 2010; Alkroosh and Nikraz 2012).

In recent years, AIs have been used with varying degrees of success for prediction of axial and lateral bearing capacities of pile foundations in compression and uplift, including driven piles (Chan et al. 1995; Goh 1996;Lee and Lee 1996; Teh et al. 1997; Abu-Kiefa 1998; Goh et al. 2005; Das and Basudhar 2006;Pal 2006;Shahin and Jaksa 2006;Ahmad et al. 2007;Ardalan et al. 2009;Shahin 2010;Alkroosh and Nikraz 2011) and drilled shafts (Goh et al. 2005; Shahin 2010; Alkroosh and Nikraz 2011).

In the present study the side resistance of drilled shaft has been modeled using artificial intelligence. An error comparison has been made between different models in terms of coefficient of correlation and other statistical errors. Finally sensitivity analysis has been carried out to know the importance of parameters that influences the output in the model.

6.2 Database used in present study

Using the database of Goh et al. 2005, this problem has been reanalyzed using LS-SVM and MARS. The database was compiled from 127 field load tests on drilled shafts in a variety of cohesive soil profiles.

6.3 Database preprocessing

The database has been normalized between 0 to 1 for LS-SVM model by using the formula:

$$X_n = \frac{X - X_{\min}}{X_{\max} - X_{\min}}$$

For MARS modeling, the actual database has been used.

Table 6.1 Training dataset used in the modelling

Sl. No.	σ	S_u	α	α-value
1	53	53	0.6	-1.186
2	125	351	0.36	0.299
3	100	107	0.47	-0.098
4	29	178	0.26	-0.226
5	97	108	0.4	-0.764
6	59	57	0.72	0.153
7	29	100	0.35	-1.569
8	82	112	0.52	0.428
9	34	32	0.74	-0.495
10	126	164	0.41	-0.066
11	97	212	0.49	1.158
12	50	96	0.5	-0.374
13	34	26	0.88	0.699
14	162	130	0.44	-0.205
15	120	180	0.37	-0.332
16	17	32	0.83	0.614
17	109	94	0.54	0.365
18	30	137	0.27	-0.973
19	25	105	0.49	-0.002
20	80	117	0.37	-0.868
21	70	215	0.32	-0.082
22	34	64	0.67	-0.067
23	83	208	0.41	0.576
24	343	285	0.38	-0.196
25	95	309	0.27	-0.546
26	17	32	0.79	0.231
27	76	143	0.33	-0.612
28	120	242	0.28	-0.991
29	70	119	0.54	0.830
30	45	118	0.35	-0.924
31	57	45	0.83	0.760
32	19	307	0.24	-0.478
33	23	112	0.39	-0.670
34	34	166	0.33	0.244
35	119	303	0.42	0.752

Sl. No.	σ	S_u	α	α-value
51	83	208	0.34	-0.094
52	74	115	0.5	0.319
53	37	102	0.61	0.969
54	44	182	0.42	1.191
55	79	51	1.03	3.219
56	60	140	0.31	-0.730
57	28	80	0.8	1.888
58	48	266	0.38	0.754
59	70	226	0.3	-0.278
60	102	71	0.54	-0.326
61	25	68	0.67	0.164
62	105	120	0.42	-0.287
63	45	109	0.38	-0.980
64	60	186	0.25	-0.645
65	80	96	0.33	-1.906
66	30	132	0.28	-1.033
67	67	136	0.45	0.455
68	34	32	0.72	-0.686
69	25	68	0.63	-0.219
70	57	53	0.7	-0.204
71	70	94	0.51	-0.320
72	200	113	0.62	1.238
73	29	165	0.27	-0.311
74	125	375	0.34	0.051
75	53	42	0.73	-0.325
76	127	389	0.32	-0.232
77	18	95	0.61	0.771
78	83	193	0.37	0.169
79	67	123	0.5	0.578
80	19	307	0.25	-0.382
81	40	45	0.7	-0.523
82	37	126	0.51	0.934
83	83	192	0.37	0.167
84	82	117	0.49	0.282
85	197	105	0.36	-1.194

36	40	57	0.66	-0.469
37	29	74	0.57	-0.577
38	55	147	0.33	-0.328
39	109	106	0.48	0.041
40	97	96	0.45	-0.593
41	105	340	0.29	-0.265
42	37	126	0.37	-0.406
43	113	178	0.48	0.793
44	36	43	0.78	0.197
45	70	94	0.68	1.308
46	26	179	0.25	-0.291
47	57	58	0.64	-0.590
48	34	74	0.58	-0.512
49	110	297	0.27	-0.678
50	37	168	0.39	0.822

86	102	65	0.59	-0.007
87	43	21	0.83	0.057
88	28	80	0.76	1.505
89	63	56	0.83	1.209
90	160	260	0.39	-0.205
91	25	125	0.41	-0.003
92	164	153	0.53	0.632
93	102	70	0.55	-0.257
94	28	47	0.79	0.496
95	34	86	0.63	0.486
96	100	94	0.49	-0.227

6.4 Different developed model equations

The different model equations developed from SVM and MARS are presented in the next segments.

6.4.1 LS-SVM Model equation

For the LS-SVM model, Radial basis kernel function has been used for transformation of the inputs. The optimum values of bias, regularization parameter and with of radial basis function is given below and the value for Lagrange multiplier for all the inputs has been represented in Figure 6.1: b = -0.2303, γ=1.7155, σ^2=1.9817

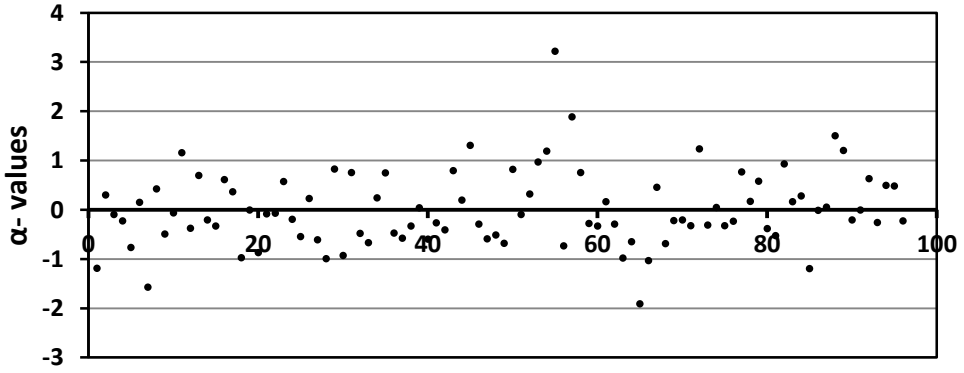

Figure 6.1 Optimum values of Lagrange multiplier (α)

6.4.2 MARS model equation

For developing the MARS, 13 basis functions have been introduced in forward phase and in backward elimination phase, 4 basis functions have been removed from the MARS model. So, the final MARS contains 9 basis functions. The ideal MARS model is given below

$$BF_1 = \max(0, S_u - 132)$$

$$BF_2 = \max(0, 132 - S_u)$$

$$BF_3 = \max(0, 160 - \sigma)$$

$$BF_4 = BF_2 \times \max(0, \sigma - 79)$$

$$BF_5 = BF_2 \times \max(0, 79 - \sigma)$$

$$BF_6 = BF_4 \times \max(0, 82 - \sigma)$$

$$BF_7 = BF_5 \times \max(0, \sigma - 28)$$

$$BF_8 = \max(0, 132 - S_u) \times \max(0, \sigma - 79) \times \max(0, \sigma - 82) \times \max(0, S_u - 105)$$

$$BF_9 = BF_4 \times \max(0, 109 - \sigma)$$

$$\alpha = 0.453 - 0.000388 \times BF_1 + 0.00813 \times BF_2 - 0.000887 \times BF_3 - 0.000107 \times BF_4 - 5.45e\text{-}5 \times BF_5 - 0.0044 \times BF_6 - 3.93e\text{-}6 \times BF_7 + 1.14e\text{-}7 \times BF_8 - 1.98e\text{-}5 \times BF_9 \quad (6.1)$$

6.5 Result comparison

The statistical performances i.e. Mean Absolute Error (MAE), Root Mean Squared Error (RMSE), Correlation Coefficient (R) and coefficient of efficiency (R^2) for the model are presented in Table 6.2.

The results of MARS have been matched with ANN (Goh et al., 2005) and LS-SVM model established. The assessments have been done in terms of Mean Absolute Percentage Error (MAPE), and Root Mean Square Error (RMSE). Figure 6.2 and 6.3 depict the bar chart of MAPE and RMSE for training dataset, respectively and it is observed that the developed MARS outperform ANN and LS-SVM models. Studies emphasized that regression equations obtained by the MARS technique make robust and coherent parameter valuations. From

Figure 6.4, the performance of MARS model can be observed. Figure 6.5 represents the variations in actual and predicted value of the training dataset taken in the present study.

Table 6.2 Performances of different models

Model	Model Inputs		RMSE	MAPE	Correlation coefficient (R)	Coefficient of determination (R^2)
Model I	**Goh et al. (2005)**	**Training**	0.078	13.14	0.91	0.81
		Testing	0.074	13.9	0.86	0.8
Model II	**SVM**	**Training**	0.08	13.27	0.9	0.8
		Testing	0.08	16.3	0.88	0.77
Model III	**MARS**	**Training**	0.06	11.28	0.935	0.84
		Testing	0.06	10.47	0.94	0.8

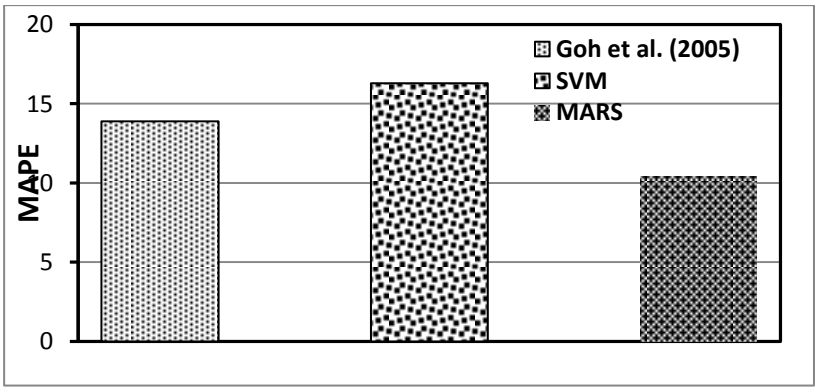

Figure 6.2 Comparison between models in terms of MAPE

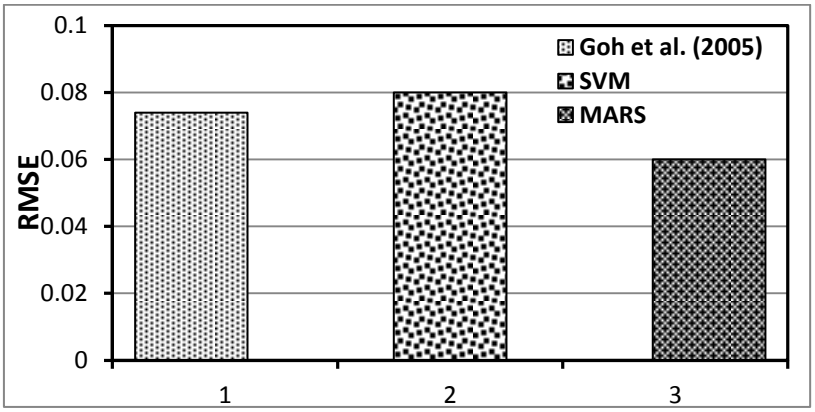

Figure 6.3 Comparison between models in terms of RMSE

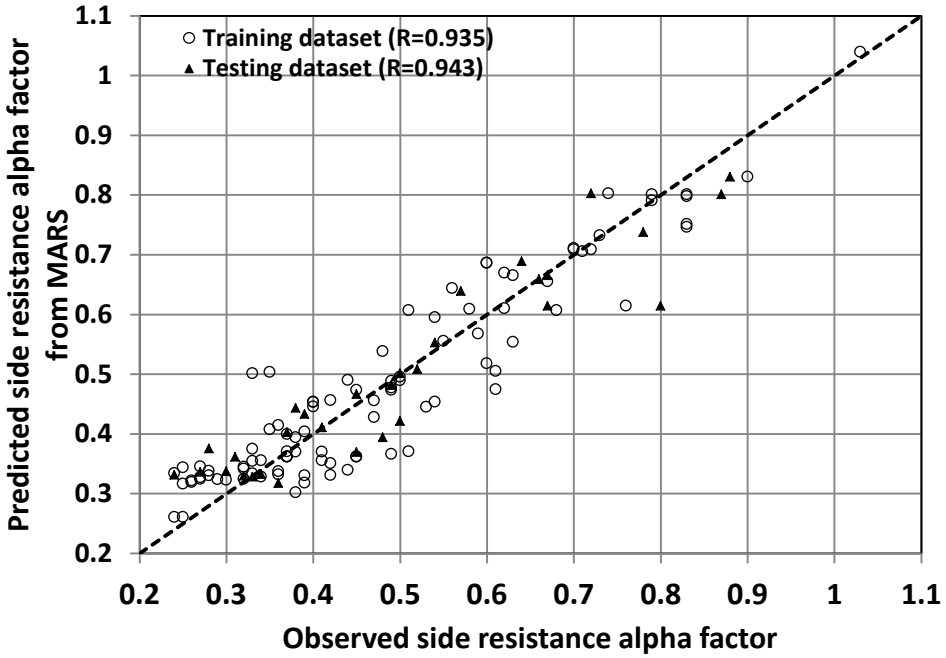

Figure 6.4 Performance of MARS model in the prediction

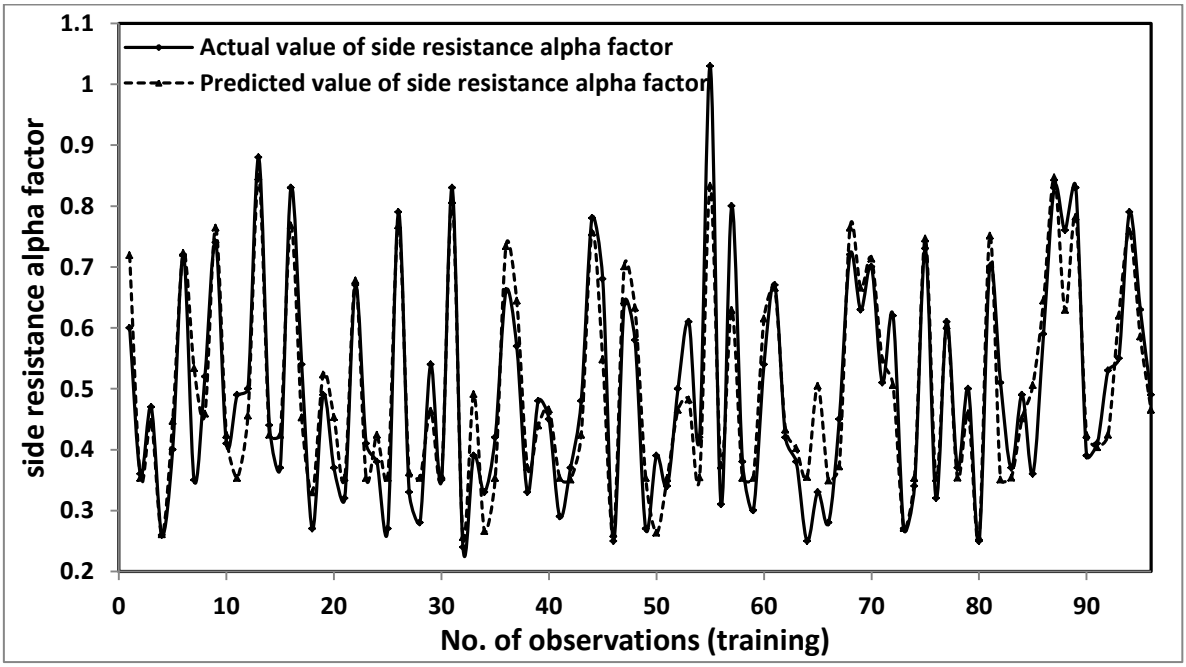

Figure 6.5 Comparison between observed and predicted values

6.6 Sensitivity of the parameters

The sensitivity tests are carried out to determine the relative significance of each of the inputs and to find the inputs that affect the models performance. The sensitivity test is carried out on the all data by varying each of the input, one at a time, at a constant rate of

20%. For every input, the percentage change in the output is observed. The sensitivity (*S*) of each input is calculated by the following:

$$S = \frac{1}{N}\sum\left(\frac{\%\ \ change\ in\ output}{\%\ \ change\ in\ input}\right)\times 100$$

where *N* = number of datasets used in the study.

The sensitivity of the parameters has been represented in Figure 6.6 and it is found that the effective overburden pressure affects the output very significantly.

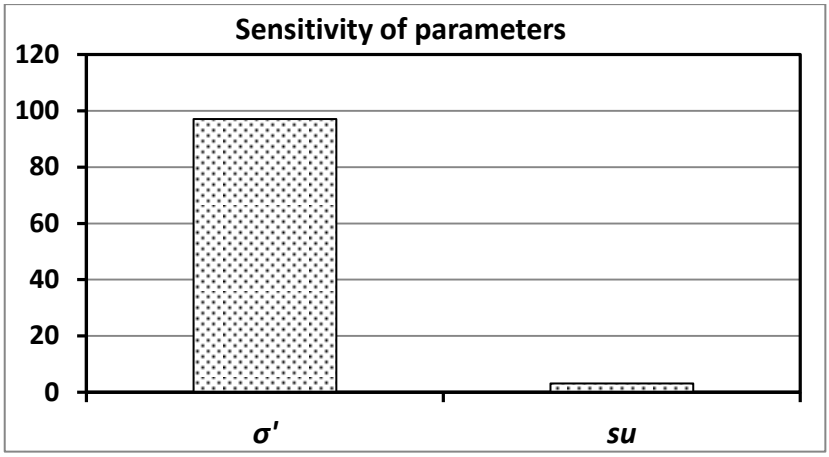

Figure 6.6 Results of sensitivity analysis

6.7 Discussion

Present study shows that the MARS model can be used to predict the side resistance of the drilled shaft. The model shows a correlation coefficient of 0.93 in training with a mean absolute percentage error of 11.28 which is lower when compared with the literature. The overburden pressure affects the model very significantly; hence it is desirable to determine the overburden pressure precisely in the field.

CHAPTER 7
CONCLUSION AND FUTURE SCOPE

7.1 Conclusion

Present study focuses on the use of ANN, SVM and MARS in modeling four geotechnical problems. The first problem deals with the prediction of compaction parameters (i.e. MDD and OMC) of sandy soil. Out of the three models the MARS model gives better predictability and sensitivity analysis shows that the coefficient of uniformity and percentage of sand affects the model very significantly. The second problem deals with the prediction of relative density (D_r) of clean sand. The predictability of LS-SVM is found to be very accurate when compared to other methods and coefficient of uniformity and mean grain size are found to be the important parameters affecting the model. Third problem deals with the prediction of compression index of clay and developed ANN outperforms than SVM and MARS. In this case liquid limit, plasticity index and natural moisture content affect the model significantly. The fourth model deals with the prediction of side resistance of drilled shaft and the MARS model performs better than the other models. Sensitivity analysis shows that the effective stress affects the model severely. The resultant predictions of different output parameters by the different models agree well with the available experimental data. Although prediction error limits were often large, estimation of those parameters with soft computing may be accurate enough for most applications, and hence will fill a need where the physical parameters are not readily available. These techniques may also provide new approaches and methodologies and minimize the potential variation of correlations. Therefore, the practical outcome of the proposed models could be used with acceptable accuracy at the preliminary stage of design.

7.2 Future scope for research

The evaluation of the established models indicates that the capability of different

technique rest on the type of problem and the complexity of the database. Further researches can be done in the area of data division into training and testing, validation of models conducting laboratory experiments, appropriate method for sensitivity analysis to determine the significance of the input parameters. As these techniques applicable within a specific range of inputs and outputs, other techniques (i.e. genetic programming, ANFIS, Relevance Support Vector Machine (RVM), regression tree, principal component analysis (PCA) etc.) can be used to extrapolate the predictors and generate simplified model equations.

REFERENCES

Acciani, C., Fucilli, V., & Sardaro, R. (2011), "Data mining in real estate appraisal: a model tree and multivariate adaptive regression spline approach", *Pubblicazioni Ce. SET*, 27-45.

Ahadian, J., Ebn, J. R., & Shafaei Bajestan, M. A. H. M. O. U. D. (2008), "Determination of Soil Compression Index, Cc, In Ahwaz Region", *Journal Of Faculty Of Engineering (University Of Tabriz).*

Ahmad, I., Hesham El Naggar, M., & Khan, A. N. (2007), "Artificial neural network application to estimate kinematic soil pile interaction response parameters", *Soil Dynamics and Earthquake Engineering*, 27(9), 892-905.

Al-Khafaji, A. W. N., & Andersland, O. B. (1992), "Equations for compression index approximation", *Journal of geotechnical engineering*, 118(1), 148-153.

Alkroosh, I., & Nikraz, H. (2012), "Predicting axial capacity of driven piles in cohesive soils using intelligent computing", *Engineering Applications of Artificial Intelligence*, 25(3), 618-627.

Ardalan, H., Eslami, A., & Nariman-Zadeh, N. (2009), "Piles shaft capacity from CPT and CPTu data by polynomial neural networks and genetic algorithms", *Computers and Geotechnics*, 36(4), 616-625.

Ashayeri, A., Yasrebi, S. (2009), "Free-Swell and Swelling Pressure of Unsaturated Compacted Clays; Experiments and Neural Networks Modeling", *Geotech Geol Eng*, 27:137–153, Springer

Azzouz, A. S., Krizek, R. J., & Corotis, R. B. (1976), "Regression analysis of soil compressibility", *Soils and Foundations*, 16(2), June 1976, pp. 19-29.

Basheer, I. A. (2001), "Empirical modeling of the compaction curve of cohesive soil", *Canadian Geotech. J.*, 38(1), 29–45.

Behera, R. N., Patra C. R., Sivakugan N. and Das B. M. (2013), "Prediction of ultimate bearing capacity of eccentrically inclined loaded strip footing by ANN, part I", *International Journal of Geotechnical Engineering*, 2013 vol7 no1, page 36-44.

Boger, Z., and Guterman, H. (1997), "Knowledge extraction from artificial neural network models", *IEEE Systems, Man, and Cybernetics Conference*, Orlando, FL, USA.

Chan, W. T., Chow, Y. K., & Liu, L. F. (1995), "Neural network: an alternative to pile driving formulas", *Computers and geotechnics*, 17(2), 135-156.

Cozzolino, V. M. (1961), "Statistical forecasting of compression index", In*Proceedings of the 5th International Conference on Soil Mechanics and Foundation Engineering Paris* (Vol. 1,

pp. 51-53).

Das, S. K., Basudhar, P. K. (2008), "Prediction of Residual Friction Angle Of Clays Using Artificial Neural Network", *Engineering Geology*, Volume 100, Issue 3-4, September 2008, Pages 142-145.

Farroq, Mujtaba., Das,B. M., Sivakugan, N. (2013), "Correlation between gradational parameters and compaction characteristics of sandy soils", *International Journal of Geotechnical Engineering, 7*(4), 395-401.

Friedman, J. H. (1991), "Multivariate adaptive regression splines", The annals of statistics, 1-67.

Goh, A. T. C., Kulhawy, F. H., and Chua, C. G. (2005), " Bayesian neural network analysis of undrained side resistance of drilled shafts", *J. of Geotech. and Geoenv. Engineering*, ASCE, 131 No 1, 84-93.

Goh, A. T. C. (1995), "Modeling soil correlations using neural network", *J. Comput. Civ. Eng.*, 9(4), 275–278.

Gunaydm, O. (2009), "Estimation of soil compaction parameters by using statistical analyses and artificial neural networks", *Environ Geol,* 57:203–215, Springer.

Hastie, T., Tibshirani, R., Friedman, J., Hastie, T., Friedman, J., & Tibshirani, R. (2009), "The elements of statistical learning", (Vol. 2, No. 1). New York: Springer.

Isik F., Ozden, G. (2013), "Estimating compaction parameters of fine- and coarse-grained soils by means of artificial neural networks", *Environ Earth Science*, 69:2287–2297, Springer.

Jekabsons, G. (2010), "Areslab: Adaptive regression splines toolbox for matlab/octave."

K. Pelckmans, J.A.K. Suykens, T. Van Gestel, J. De Brabanter, L. Lukas, B. Hamers, B. De Moor, J. Vandewalle. LS-SVMlab : a Matlab/C toolbox for Least Squares Support Vector Machines, http://www.esat.kuleuven.ac.be/sista /lssvmlab .

Kalantary, F., & Kordnaeij, A. (2012), "Prediction of compression index using artificial neural network", *Scientific Research and Essays*, 7(31), 2835-2848.

Karsoliya, Saurabh (2012), "Approximating Number of Hidden layer neurons in Multiple Hidden Layer BPNN Architecture.", *International Journal of Engineering Trends and Technology*- Volume3 Issue6- 2012.

Kiefa, M. A. (1998), "General regression neural networks for driven piles in cohesionless soils", *Journal of Geotechnical and Geoenvironmental Engineering*, 124(12), 1177-1185.

Koppula, S. D. (1981), "Statistical estimation of compression index", *ASTM Geotechnical Testing Journal*, 4(2).

Korfiatis, G. P., & Manikopoulos, C. N. (1982), "Correlation of maximum dry density and grain size", *Journal of the Geotechnical Engineering Division*,108(9), 1171-1176.

Lee, I. M., & Lee, J. H. (1996), "Prediction of pile bearing capacity using artificial neural networks", *Computers and Geotechnics*, 18(3), 189-200.

Leong, E. C., Rahardjo, H., Tinjum, J. M., Benson, C. H., & Blotz, L. R. (1999), "Soil-Water Characteristic Curves for Compacted Clays", *Journal of Geotechnical and Geoenvironmental Engineering*, 125(7), 629-630.

Mollahasani, A., Alavi, A. H., Gandomi, A. H., Rashed, A. (2011), "Nonlinear Neural-Based Modeling of Soil Cohesion Intercept", *KSCE Journal of Civil Engineering* (2011) 15(5):831-840, Springer.

Mujtaba, H., Farooq, K., Sivakugan, N., & Das, B. M. (2013), "Correlation between gradational parameters and compaction characteristics of sandy soils", *International Journal of Geotechnical Engineering*, 7(4), 395-401.

Nelder, J. A., & Mead, R. (1965), "A simplex method for function minimization", *Computer journal*, 7(4), 308-313.

Nishida, Y. (1956), "A brief note on compression index of soil", *Journal of Soil Mechanics and Foundation Engineering*, ASCE, 82(3), 1-14.

Omar, M., Shanableh, A., Basma, A., & Barakat, S. (2003), "Compaction characteristics of granular soils in United Arab Emirates", *Geotechnical & Geological Engineering*, 21(3), 283-295.

O'Neill, M. W., & Reese, L. C. (1999), "Drilled shafts: Construction procedures and design methods"

Ozer, M., Isik, N. S., Orhan, M. (2008), "Statistical and neural network assessment of the compression index of clay-bearing soils", *Bulletin Engineering Geo Environ*, 67:537–545.

Pal, M., & Deswal, S. (2010), "Modelling pile capacity using Gaussian process regression", *Computers and Geotechnics*, 37(7), 942-947.

Park, H. I., & Lee, S. R. (2011), "Evaluation of the compression index of soils using an artificial neural network", *Computers and Geotechnics*, 38(4), 472-481.

Patra, C., Sivakugan, N., & Das, B. (2010), "Relative density and median grain-size correlation from laboratory compaction tests on granular soil", *International Journal of Geotechnical Engineering*, 4(1), 55-62.

Patra, C., Sivakugan, N., Das, B., & Rout, S. (2010), "Correlations for relative density of clean sand with median grain size and compaction energy", *International Journal of Geotechnical Engineering*, 4(2), 195-203.

Pooya Nejad, F., Jaksa, M. B., Kakhi, M., & McCabe, B. A. (2009), "Prediction of pile settlement using artificial neural networks based on standard penetration test data", *Computers and Geotechnics*, 36(7), 1125-1133.

Rashidian, V. and Hassanlourad, M. (2013), "Application of Artificial Neural Network for modeling the Mechanical Behavior of Carbonate Soils", *International Journal of Geomechanics*. ASCE.

Reese, L. C., Isenhower, W. M., & Wang, S. T. (2006) *Analysis and design of shallow and deep foundations* (Vol. 10). Hoboken, NJ: Wiley.

Rendon-Herrero, O. (1980), "Universal compression index equation", *Journal of the Geotechnical Engineering Division*, 106(11), 1179-1200.

Samui, P., Das, S. K., Kim, D. and Yoon, G. L. (2011), "Determination of Compression Index For Marine Clay: A Least Square Support Vector Machine Approach", *Int. J. Advance. Soft Comput. Appl.*, Vol. 3, No. 1, March 2011, ISSN 2074-8523.

Shahin, M. A. (2000), "State of the Art of Artificial Neural Networks in Geotechnical Engineering", *EJGE*, Bouquet 08.

Shahin, M. A. (2010), "Intelligent computing for modeling axial capacity of pile foundations", *Canadian Geotechnical Journal*, 47(2), 230-243.

Shahin, M. A. (2013), "Load-Settlement Modeling of Axially Loaded Drilled Shafts using CPT-Based Recurrent Neural Networks", *International Journal of Geomechanics*.

Sinha, S. K., Wang, M. C. (2008), "Artificial Neural Network Prediction Models for Soil Compaction and Permeability", *Geotech Geol Eng*, 26:47–64, Springer.

Sivrikaya, O., Togrol, E., & Kayadelen, C. (2008). "Estimating compaction behavior of fine-grained soils based on compaction energy", *Canadian Geotechnical Journal*, 45(6), 877-887.

Sivrikiya, O. (2008), "Models of compacted fine-grained soils used as mineral liner for solid waste", *Environmental Geology*, 53(7), 1585-1595.

Skempton, A. W. (1959), "Cast in-situ bored piles in London clay",*Geotechnique*, 9(4), 153-173.

Skempton, A. W., & Jones, O. T. (1944), "Notes on the compressibility of clays", *Quarterly Journal of the Geological Society*, 100(1-4), 119-135.

Smith, G. N. (1986), "Probability and statistics in civil engineering: an introduction", London: Collins.

Scholkopf, B., & Smola, A. J. (2002), "Learning with kernels: Support vector machines, regularization, optimization, and beyond", MIT press.

Suykens, J. A. K., Lukas, L., and Vandewalle, J. (2000), "Sparse approximation using least

squares support vector machines", Proceedings of the *IEEE International Symposium on Circuits and Systems* (ISCAS 2000), 2, 757–760.

Suykens, J.A.K. , Gestel, T. V., Brabanter, J. D., Moor, B. D., Vandewalle, J. (2002), "Least Squares Support Vector Machines", *World Scientific*, Singapore, 2002.

Teh, C. I., Wong, K. S., Goh, A. T. C., & Jaritngam, S. (1997), "Prediction of pile capacity using neural networks", *Journal of Computing in Civil Engineering*, 11(2), 129-138.

Tekin, E., Akbas, S.O. (2011), "Artificial neural networks approach for estimating the groutability of granular soils with cement-based grouts", *Bull Eng Geol Environ*, 70:153–161.

Tomlinson, M. J. (1957), "The adhesion of piles driven in clay soils", In *Proceedings of the 4th international conference on soil mechanics and foundation engineering*, London.

Vapnik, V. 1995. The nature of statistical learning theory, Springer, New York.

Vapnik, V. N. 1998. Statistical learning theory, Wiley, New York.

Vapnik, V., & Lerner, A. J. (1963), "Generalized portrait method for pattern recognition", *Automation and Remote Control*, *24*(6), 774-780.

Vert, Jean-Philippe, Koji, Tsuda, and Bernhard, Scholkopf (2004), "A primer on kernel methods." *Kernel Methods in Computational Biology*.

Wang, M. C., & Huang, C. C. (1984), "Soil compaction and permeability prediction models", *Journal of Environmental Engineering*, 110(6), 1063-1083.

Yilmaz, I., Marschalko, M., Bednarik, M. (2012), "Neural computing models for prediction of permeability coefficient of coarse-grained soils", *Neural Comput & Applic*, 21:957–968, Springer.

Yin-Wen Chang, Cho-Jui Hsieh, Kai-Wei Chang, Michael Ringgaard and Chih-Jen Lin (2010), "Training and testing low-degree polynomial data mappings via linear SVM.", *J. Machine Learning Research* 11:1471–1490.

Yusuf, E., Gul, T. O. (2012), "The use of neural networks for the prediction of the settlement of one-way footings on cohesionless soils based on standard penetration test", *Neural Comput & Applic*, December 2012, Springer.